AD_____

Award Number: W81XWH-10-2-0053

TITLE: Vesicant Therapeutics Collaborative Core Research Program

PRINCIPAL INVESTIGATOR: Hai-Quan Mao, Ph.D.

CONTRACTING ORGANIZATION: Johns Hopkins University
Baltimore, Maryland 21218

REPORT DATE: December 2012

TYPE OF REPORT: Final

PREPARED FOR: U.S. Army Medical Research and Materiel Command
Fort Detrick, Maryland 21702-5012

DISTRIBUTION STATEMENT: Approved for Public Release;
Distribution Unlimited

REPORT DOCUMENTATION PAGE

Form Approved
OMB No. 0704-0188

1. REPORT DATE	2. REPORT TYPE	3. DATES COVERED
December 2012	Final	01/June/2010–30/November/2012

4. TITLE AND SUBTITLE

Vesicant Therapeutics Collaborative Core Research Program

5a. CONTRACT NUMBER

5b. GRANT NUMBER
W81XWH-10-2-0053

5c. PROGRAM ELEMENT NUMBER

6. AUTHOR(S)

Hai-Quan Mao, Ph.D.

E-Mail: hmao@jhu.edu

5d. PROJECT NUMBER

5e. TASK NUMBER

5f. WORK UNIT NUMBER

7. PERFORMING ORGANIZATION NAME(S) AND ADDRESS(ES)

Johns Hopkins University

Baltimore, Maryland 21218

8. PERFORMING ORGANIZATION REPORT NUMBER

9. SPONSORING / MONITORING AGENCY NAME(S) AND ADDRESS(ES)

U.S. Army Medical Research and Materiel Command
Fort Detrick, Maryland 21702-5012

10. SPONSOR/MONITOR'S ACRONYM(S)

11. SPONSOR/MONITOR'S REPORT NUMBER(S)

12. DISTRIBUTION / AVAILABILITY STATEMENT

Approved for Public Release; Distribution Unlimited

13. SUPPLEMENTARY NOTES

14. ABSTRACT

This project at Johns Hopkins University serves as the In Vivo Delivery System Development Core of the Phase I Vesicant Therapeutics Collaborative Core Research Program (VT-CCRP). The Mission of this Core is focused on achieving Aim 3 of the Parent Grant at the USAMRICD. This Core aims to develop, evaluate, and downselect a nanotechnology-based system for in vivo RNAi delivery. This will be a critical component of validating therapeutic targets identified by the Target Discovery and In Vitro Validation Core in in vivo models of vesicant exposure.

15. SUBJECT TERMS none provided

16. SECURITY CLASSIFICATION OF:			17. LIMITATION OF ABSTRACT	18. NUMBER OF PAGES	19a. NAME OF RESPONSIBLE PERSON
a. REPORT	b. ABSTRACT	c. THIS PAGE			USAMRMC
U	U	U	UU		19b. TELEPHONE NUMBER *(include area code)*

Table of Contents

Introduction

This project at Johns Hopkins University serves as the In Vivo Delivery System Development Core of the Phase I Vesicant Therapeutics Collaborative Core Research Program (VT-CCRP). The Mission of this *Core* is focused on achieving Aim 3 of the Parent Grant at the USAMRICD. **This Core aims to develop, evaluate, and downselect a nanotechnology-based system for *in vivo* RNAi delivery.** This will be a critical component of validating therapeutic targets identified by the *Target Discovery and In Vitro Validation Core* in *in vivo* models of vesicant exposure.

The Specific Aims are to evaluate nanotechnology-based delivery systems for RNAi delivery, to confirm delivery to target tissues *in vivo*, confirm knockdown of target *in vivo*, and to select the most effective delivery system for validation of targets *in vivo*. Two delivery systems, chitosan nanoparticles and PEG-PPA nanoparticles, will be under development and evaluation.

The proposed tasks are:

(i). Develop chitosan/siRNA nanoparticles and PEG-PPA/siRNA nanoparticles with well characterized biophysical properties.
(ii). Characterize nanoparticle activities *in vitro* and identify the most effective nanoparticle formulation for each type of target cells.
(iii). Develop an imiquimod cream-based nanoparticle formulation for animal experiments testing transdermal delivery efficacy (to be conducted at USAMRICD).
(iv). Confirm delivery to target tissues and knockdown of target though intranasal instillation in mouse and rat models.
(v). Confirm delivery to target tissue and knockdown of target for ocular delivery.

At the advise by USAMRMC and VT-CCRP at USAMRICD, we abandoned items (iii) and (iv), and focused on nanoparticle assembly and ocular delivery only. Therefore, the revised tasks are:

(i). Develop chitosan/siRNA nanoparticles and PEG-PPA/siRNA nanoparticles with well characterized biophysical properties.
(ii). Characterize nanoparticle activities *in vitro* and identify the most effective nanoparticle formulation for each type of target cells.
(iii). Confirm delivery to target tissue and knockdown of target for ocular delivery.

Body

In Phase I of the Delivery System Development Core, we have developed siRNA micellar nanoparticle systems prepared from cationic copolymer carriers including poly(ethylene glycol-*b*-phosphoramidate) (PEG-*b*-PPA) copolymers, and graft copolymers of linear polyethyleneimines and polyethylene glycol (PEG). Two important approaches were developed to effectively condense siRNA to small and uniform nanoparticles (~50 nm) and to markedly enhance the colloidal and complex stability of siRNA in in physiological buffer and serum-containing media. These properties have been correlated with significantly improved siRNA delivery and gene knockdown efficiency (70–80%).

We will then summarize the key findings in the report here. Just to clarify at the outset that we quickly tested the efficiency of chitosan-siRNA nanoparticles and found that the transfection and gene knockdown efficiency is much lower than linear PEI/siRNA and PPA/siRNA nanoparticles. Thus, we focused on two most effective nanoparticle systems we have screened.

1. PEG-*b*-PPA ternary nanoparticles with improved condensation ability and uniform particle size

Nanoparticle Synthesis. Despite of the success of mediating DNA delivery, compacting siRNA with polymeric carrier into distinct, small and stable nanoparticles has been challenging due to the much lower molecular weight and condensation ability of siRNA as compared with plasmid DNA. We have developed a convenient method to enhance the condensation between PEG-*b*-PPA and siRNA with sodium tripolyphosphate (TPP) via ionic crosslinking (Fig. 1).[32] Smaller and more uniform nanoparticles were formed in relatively low concentration of TPP at lower N/P ratios. The major advantages of TPP as a stabilization crosslinker is low toxicity nature of TPP (an inert small molecular weight salt, widely used as food additive, and on FDA's generally regarded as safe–GRAS–list) and the convenience of simply mixing TPP and siRNA solution before complexing with PEG-*b*-PPA solution. TPP was first used to prepare chitosan nanoparticles by forming ionic crosslinks between positively charged amino groups of chitosan and negatively charged phosphates in TPP.[33,34] Among many polyanionic crosslinkers investigated, TPP is the most popular for chitosan crosslinking because of its non-toxic nature and effective crosslinking ability. In addition, the inclusion of TPP did not interference with the complexation between PEG-*b*-PPA and siRNA.

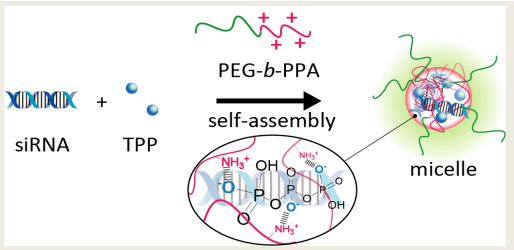

Fig. 1. Schematic of preparation of PEG-*b*-PPA/siRNA/TPP ternary micellar nanoparticles formed through ionic crosslinking with sodium tripolyphosphate (TPP).

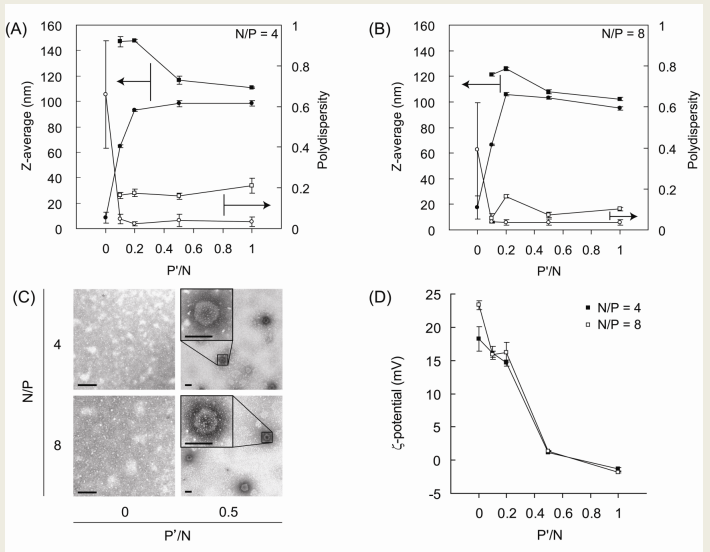

Fig. 2. The z-average (left ordinate) and PDI (right ordinate) measured by dynamic light scattering analysis of nanoparticles formed at various P'/N ratios and N/P ratios of 4 (A) and 8 (B), respectively, before (●, ○) and after (■, □) incubation with 150 mM NaCl for 5 hours. Values represent Mean ± SEM (n = 3). (C) TEM images of nanoparticle formed at P'/N ratios of 0 and 0.5 for N/P ratios of 4 and 8, respectively. (D) Zeta-potential of nanoparticles prepared at various P'/N ratios for N/P ratios of 4 (■) and 8 (□), respectively. Values represent Mean ± SEM (n = 3).

Although PEG-*b*-PPA and siRNA formed complexes at N/P ratios of 4 and 8, particles were irregular shaped with wide size distribution (Fig. 2). The addition of TPP drastically improved the condensation

efficiency, forming spherical nanoparticles with small and distinct sizes at P'/N ratio as low as 0.2. The mechanism of enhanced condensation is likely through intermolecular electrostatic interaction, due to the multivalent anionic nature of TPP. PEG-*b*-PPA solutions were incubated with a mixture of siRNA and TPP at N/P ratios (the molar ratio of total side-chain amino groups in PEG-*b*-PPA to phosphates in siRNA) of 4 and 8 and a variety of P'/N ratios (the molar ratio of phosphate groups to side-chain amino groups in PEG-*b*-PPA) to form polyelectrolyte complexes (Fig. 2). At P'/N ratio of 4–8, there is no significant particle formation (z-average size < 10 nm) with large PDI. On the other hand, gel electrophoresis analysis showed that migration of siRNA was retarded or retained at the same set of N/P and P'/N ratios (Fig. 3A and D). These results indicate that siRNA could only bind to PEG-*b*-PPA strand through electrostatic interaction without forming distinct particles. When TPP was used during the condensation, particle formation was observed at P'/N ratio of 0.1 or higher. The mean particle size of the assembled nanoparticles increased to 80 to 100 nm as measured by DLS (Figs. 2A, B). Of interest, PDI of nanoparticles prepared with TPP was less than 0.1 and the histogram analysis showed unimodal distribution of the nanoparticles. These data indicated that TPP was highly effective in facilitating siRNA condensation and nanoparticle formation.

The encapsulation efficiency of siRNA into nanoparticles was confirmed by agarose gel electrophoresis (Figure 3A, D). No evidence of free siRNA was seen in all the samples, including nanoparticles prepared without TPP. This result suggests good complexation ability of PEG-*b*-PPA with siRNA which does not compromise upon addition of TPP at all P'/N ratios used. At all P'/N ratios tested TPP was not found replace siRNA from the polymer. To test whether addition of TPP would cause replacement of siRNA from the polymer we carried out agarose gel electrophoresis (Figure 3A, D). No evidence of free siRNA suggested that complexation ability of PEG-*b*-PPA with siRNA does not compromise upon addition of TPP at all P'/N ratios used.

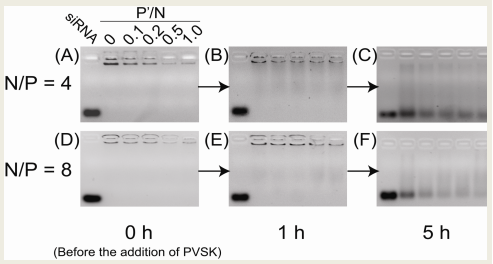

Fig. 3. Gel retardation assay of complexation efficiency for siRNA at various P'/N ratios for N/P ratios of 4 and 8, respectively. Nanoparticles prepared at various conditions were incubated with PVSK for 1 and 5 hours at 37 °C at a molar ratio of sulfate groups in PVSK to phosphate groups in siRNA of 5.

Significant differences in particle morphology were also observed in transmission electron microscopy (TEM) analysis between nanoparticle preparations in the presence and absence of TPP. TEM images of nanoparticles prepared with TPP showed that these particles were mostly spherical with diameters ranging from 80 to 100 nm (Figure 2C), corroborated well with the average size (98.2 ± 10.2 nm) measured by DLS method. On the other hand, the TEM images of particles formed without TPP revealed aggregates with irregular shape and sized ranged from 20 to 100 nm, correlated with higher PDI. Nanoparticles with TPP showed much higher contrast than that without TPP in TEM images, indicating that the TPP-condensed nanoparticles may have more compact polyplex core than that without TPP.

The most striking consequence of TPP co-condensation is the change in nanoparticle surface charge (Fig. 3D). The ζ-potential of the ternary nanoparticles reduced drastically to neural at a P'/N ratio of 0.5. This may significantly impact the *in vivo* nanoparticle transport and stability, as positively charged nanoparticles are prone to opsinization and passive adsorption with abundant negatively charged serum proteins, leading to particle aggregation and uptake by macrophages.

Enhanced stability of nanoparticles at physiological ionic strength. The complex stability of nanoparticles was assessed by monitoring changes in size, PDI and SLI of nanoparticles prepared with lower P'/N ratios (0.1-0.2) showed much larger sizes after incubating in 0.15 M NaCl, whereas at higher P'/N ratios there were only slightly increases in average particle size (~110 and ~100 nm, for N/P = 4 and 8, respectively) and low PDI. In addition, smaller particle size increase at higher P'/N ratios was observed (Fig. 3). These data demonstrated that TPP crosslinked nanoparticles could stabilize siRNA nanoparticles in solution with physiological ionic strength.

The stability of the nanoparticles was also analyzed by characterizing the release profile of the incorporated siRNA from nanoparticles in polyanion-exchange reaction (Figs. 3B, C, E, and F).[35] There exists various types of anionic polymers including anionic proteins, sulfated polysaccharides, nuclear chromatin and messenger RNA (mRNA) as essential cellular components and exchange reaction of polycation with these negatively-charged polymers may take place under the biological environment. As a result, siRNA is released from nanoparticle through the intermolecular exchange and the released siRNA can facilitate a series of subsequent RNAi processes for gene silencing. On the other hand, nanoparticles should be sufficiently stable to resist decomplexation and release of siRNA before they reach the cytosol of target cells. Therefore, maintaining a balanced complex stability is important to successful transfection and knockdown approach.

Another advantage of the PEG-*b*-PPA/siRNA/TPP nanoparticle system is the tunable stability. The complex stability of the ternary nanoparticles was found to be dependent on N/P and P'/N ratios. The stabilization effect of TPP increased with P'/N ratio, and was more pronounced at lower N/P ratio. In general, the PEG-*b*-PPA/siRNA/TPP ternary nanoparticles were smaller and more stable at higher N/P and P'/N ratios. Based on the required stability for different gene knockdown applications, it may be possible to fine-tune the stability of the ternary nanoparticles to maintain sufficient stability for nanoparticles to transport to target cells, escape endolysosomal compartment, reach the cytosol of target cells, and allow intracellular release of siRNA in physiological ionic strength and in the presence of polyelectrolytes.

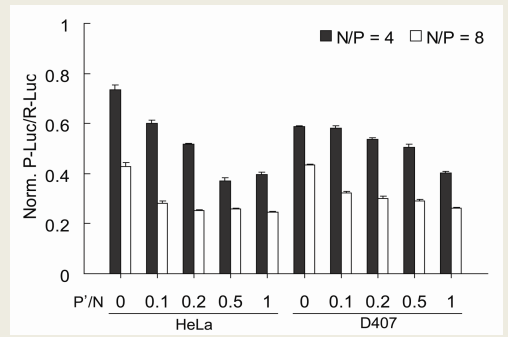

Fig. 4. Gel retardation assay of complexation efficiency for siRNA at various P'/N ratios for N/P ratios of 4 and 8, respectively. Nanoparticles prepared at various conditions were incubated with PVSK for 1 and 5 hours at 37 °C at a molar ratio of sulfate groups in PVSK to phosphate groups in siRNA of 5.

Transfection and knockdown efficiency of PPA-*b*-PPA/siRNA nanoparticles. The knockdown efficiency of PPA-*b*-PPA/siRNA nanoparticles *in vitro* was assessed in two different types of cells, human epithelial cervical cancer cells (HeLa) and human retinal pigment epithelial cells (D407) (Fig. 4). In this experiment, HeLa and D407 cells were transiently transfected respectively with the two kinds of reporter gene P-Luc and R-Luc, followed by the treatment with nanoparticles prepared at different P'/N ratios (0 to 1.0) with siRNA against P-Luc. The expression level of R-Luc was used as an internal reference for the initial transgene expression level. At 44 h after transfection, the inhibition of P-Luc expression was assayed by measuring the relative expression ratio of P-Luc/R-Luc at a concentration of 100 nM siRNA.

Although PEG-*b*-PPA/siRNA complexes without TPP mediated an average of 24% and 58% knockdown efficiency at an N/P ratio of 4 and 8, respectively, TPP-crosslinked nanoparticles resulted in higher knockdown efficiency at both N/P ratios in both cell lines. As the P'/N ratio increases, the gene knockdown efficiency increased gradually. At an N/P ratio of 4, the knockdown efficiency reached the plateau (~60%) at P'/N ratio of 0.5 in HeLa cells, and the highest at P'/N ratio of 1.0 in D407 cells. The knockdown efficiency was much higher at an N/P of 8, and was less dependent on the P'/N ratio—reached 76% for P'/N ratio of 0.2 to 1.0 in HeLa cells and 75% at P'/N ratio of 1.0 in D407 cells. Clearly, stabilization by ionic crosslinking by TPP improved nanoparticle-mediated transfection and gene knockdown efficiency.

Cytotoxicity of PEG-*b*-PPA/siRNA nanoparticles. The potential cytotoxicity of PEG-*b*-PPA/siRNA nanoparticles was assessed in HeLa cells and D407 cells under the transfection conditions. The cell viability was determined by WST assay using water-soluble tetrazolium salt (data not shown). Nearly 100% of cell viability was observed for all transfection conditions in HeLa cells, and over 90% of cell viability of D407 cells was observed under the same conditions. There was no significant difference in cell viability was observed between nanoparticles prepared with and without TPP co-condendation. These results demonstrate that the addition of TPP into nanoparticle assemblies did not influence their cytotoxicity.

2. Hyaluronic acid-coated siRNA nanoparticles–corneal-tissue targeted siRNA nanoparticles

To improve the mucoadhesive properties of the ternary nanoparticles, we conjugated hyaluronic acid (HA) to the nanoparticle surface. HA has been show to exhibit mucoadhesive and penetration enhancement properties (2). More importantly, corneal epithelial cells and limbal epithelial stem and progenitor cells express CD44, which is the receptor for HA (3-5). HA-coated or conjugated nanoparticles have been shown to significantly enhance their cellular uptake (6) via a caveolin-dependent endocytic pathway (5). Using the same TPP crosslinking strategy described above, we have optimized a protocol for preparing siRNA nanoparticles with polycation/siRNA-loaded core with HA corona for corneal delivery (Fig. 5). We used linear PEI (LPEI) and branched PEI (BPEI) as the polycation to show the versatility of this approach in applying to different polycation carriers. Here we will focus on data with LPEI, due to its high transfection activity and lower cytotoxicity.

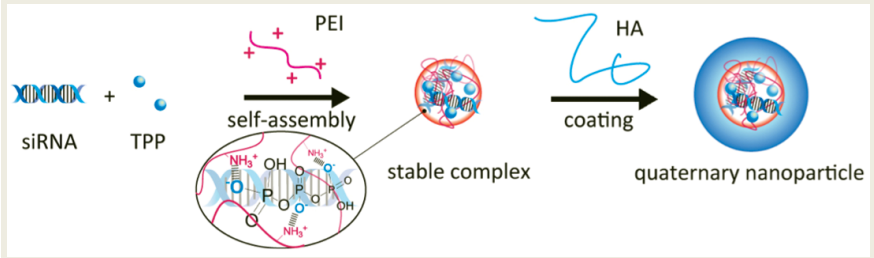

Fig. 5. Schematic illustration for synthesizing quarternary siRNA nanoparticles by coating of hyaluronic acid (HA) onto TPP-crosslinked lPEI/siRNA nanoparticles.

TPP-stabilization of the complex core. Discrete nanoparticles were prepared with N/P ratio of higher than 9 for lPEI and P'/P ratio (ratio of phosphate in TPP to phosphate in siRNA) of 4 or higher. LPEI/TPP/siRNA formed nanoparticle with positive charged surface at N/P' ratios before reaching to electroneutral mixing ratio, where large aggregates were formed. TEM images of LPEI/TPP/siRNA ternary nanoparticles showed spherical shape with diameters ranging from 70 nm to 100 nm with a unimodal distribution prior to HA coating (Fig. 6).

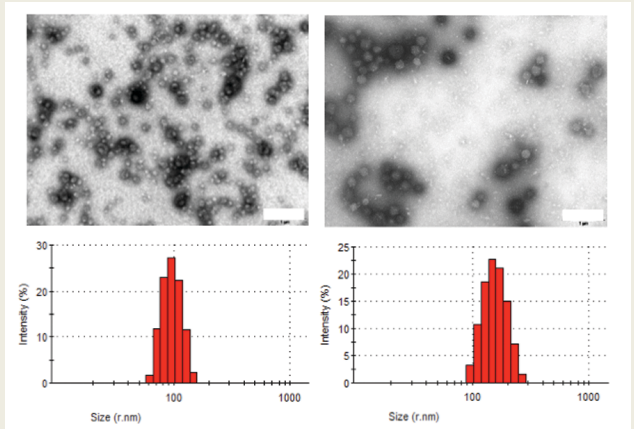

Fig. 6. TEM images and size distribution of nanoparticles prepared before (left panels) and after (right panels) HA-coating for lPEI/TPP/siRNA (charge ratio of 10:10:4:1) nanoparticles.

HA-coating confer negative surface charge to siRNA nanoparticles. HA coating can only be achieved with TPP-stabilized siRNA nanoparticles. Through optimization of HA to PEI to TPP to siRNA, we identified the range of compositions to yield stable nanoparticles. The obtained quaternary nanoparticle have the size from 90 to 120 nm in diameter. The z-potential values of near electrostatic neutrality of ternary nanoparticles with TPP sharply decreased to – 47 mV when HA to siRNA charge ratio increased from 0 to 10. Agarose gel electrophoresis revealed the encapsulation efficiency of siRNA into nanoparticles was 100%. Free siRNA was not observed for all samples including HA-coated quaternary nanoparticles, highlighting the good condensation ability and stabilization ability of TPP. The electronegative surface may be advantageous in preventing nanoparticles from aggregation when applied in physiological media.

Complex stability of nanoparticles at physiological ionic strength or in serum-containing medium. To investigate the effect of HA-coating on colloidal stability in 0.15 M of NaCl solution or in medium containing 10% serum, the colloidal stability of ternary and quaternary nanoparticles were assessed by monitoring changes in size (data not shown). No significant difference on the stability was observed between HA-uncoated and HA-coated nanoparticles in the salt solution. In salt solution, the size of nanoparticles was maintained for at least 6 h at 37°C. Ternary nanoparticles prepared with PEI showed increased sizes after incubating in 10% serum. This is probably due to the fact that positively-charged ternary nanoparticles interact with anionic serum proteins in the medium,

resulting in the aggregation. On the other hand, HA-coated quaternary nanoparticles exhibited improved colloidal stability in serum containing medium (Data not shown). HA-coated quaternary nanoparticles showed increased colloidal stability. This indicates that HA shell of TPP-stabilized nanoparticle, could stabilize siRNA nanoparticles in a solution with physiological ionic strength.

Transfection and Knockdown Efficiency of siRNA-loaded Nanoparticles was assessed in different types of cells, human epithelial cervical cancer cells (HeLa) and human corneal epithelial cells (HCE-2) and human corneal limbal epithelial cells (HCLE). These cells were selected because they express CD44. As the amount of HA/PEI/TPP increased, the gene knockdown efficiency increased up to 80 to 90% in serum-containing medium (Fig. 7a). Negatively charged quaternary nanoparticle with HA shell showed a similar level of the gene knockdown efficiency to the positively charged ternary nanoparticles. Nonetheless, these two types of nanoparticles enter the cells through different mechanisms: Cationic nanoparticles adsorbed onto negatively charged cell surface, thus triggering endocytosis, whereas HA-coated nanoparticles naturally are repelled by the electrostatic repulsion, but can bind to cells through CD44 receptor, and enter cells through CD44-HA complex-mediated endocytosis.

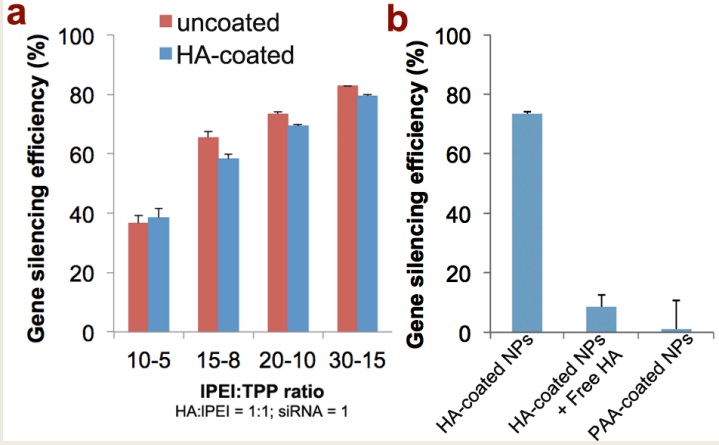

Fig. 7. TEM images and size distribution of nanoparticles prepared before (left panels) and after (right panels) HA-coating for lPEI/TPP/siRNA (charge ratio of 10:10:4:1) nanoparticles at siRNA dose of 0.6 μg/well.

To test this hypothesis that HA-coated nanoparticles show selective cellular uptake via CD44 receptor-mediated endocytosis, a competitive cell-binding assay was performed in HeLa cells. The gene knockdown efficiency of HA-coated quaternary nanoparticles was significantly reduced to ca. 10% when incubated together with 1 mg/mL concentration of free HA in culture media in HeLa cells (Fig. 7b). Furthermore, polyacrylic acid (PAA)-coated PEI/TPP/siRNA nanoparticles yielded nearly background level of transfection. These data confirmed that HA-coated nanoparticles can mediate CD44-specific cell uptake and transfection.

We next verified the transfection and knockdown efficiency of HA-coated nanoparticles in human corneal epithelial cells in HCE-2 and HCLE cells. LPEI/TPP/siRNA ternary nanoparticle with the size of 100 nm showed 35 to 50% of gene silencing efficiency and HA-coated quaternary nanoparticles showed the highest efficiency of knockdown of 65% (Fig. 8). These results again confirmed that TPP-stabilized core is important to achieving high gene silencing activity of the nanoparticles.

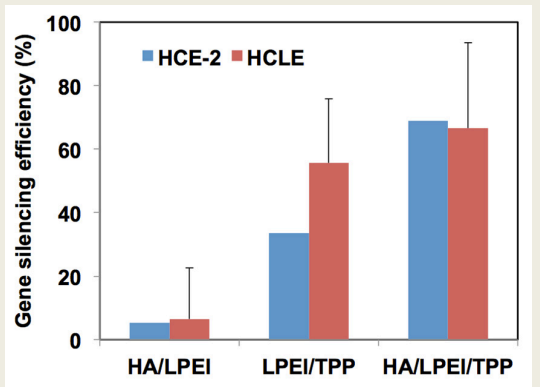

Fig. 8. Gene silencing efficiency mediated by HA-coated, siRNA(against firefly)-loaded nanoparticles (HA to PEI charge ratio = 1) in human corneal epithelial (HCE-2) cells and human corneal limbal epithelial (HCLE) cells. The dose of siRNA was 100 nM (~ 0.6 μg per well).

3. Improved siRNA condensation and transfection efficiency.

We previously developed a series of PEG-*b*-PPA block copolymers for the purpose of condensing DNA. Complexation of these copolymers with plasmid DNA yielded uniform (<100 nm), stable, self-assembled micellar nanoparticle structures. Furthermore, we have shown that the condensation of DNA can be controlled by using copolymers with different molecular weight blocks to form nanoparticles with dimensions similar to virus particles (1, 7-11). Using the same approach, we have developed a method to effective condense siRNA into small and discrete nanoparticles as small as 50 nm and rod-like particles (Fig. 9).

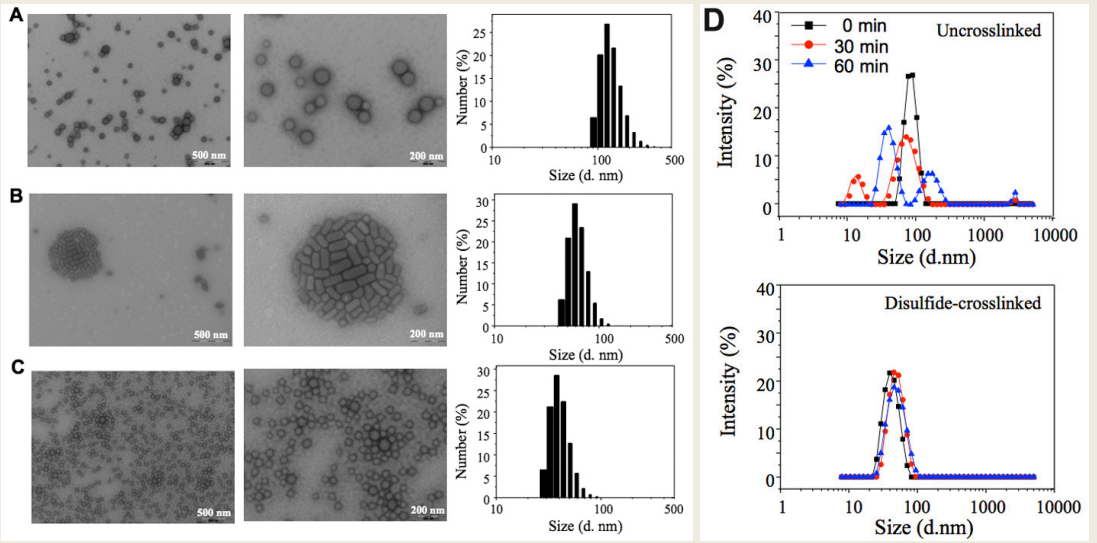

Fig. 9. The morphologies and size distribution of copolymer/siRNA nanoparticles prepared in solvents with different polarities to strengthen the condensation of siRNA and control the particle shape and size. (A) prepared in pure water; (B) prepared in water/DMF (1/1, v/v) mixture solvent; (C) prepared in water/DMF (3/7, v/v) mixture solvent. The first and second column of panels shows TEM images of the same set of samples at different magnifications. The third column of panels shows size distribution of copolymer/siRNA nanoparticles measured by dynamic light scattering (DLS). (D) Size distribution profiles of nanoparticles of these nanoparticles before (top panel) and after (lower panel) reversible disulfide crosslinking to confer the stability of the nanoparticles with incubation in 0.15 M NaCl solution measured by dynamic light scattering for nanoparticle (C).

Reversible crosslinking strategy to stabilize nanoparticles. In order to retain the shapes of the nanoparticles and also improve the stability of the nanoparticles in physiological medium, we have adopted a strategy that we developed previously for DNA nanoparticles using reversible disulfide bonds to crosslink the micelle core (Fig. 10a). We have shown that micelles prepared with this method not only retained high colloidal stability (Fig. 10b), but also released the siRNA effectively when the nanoparticles were treated with dithiothreitol (DTT), a reducing agent mimicking the function of glutathione

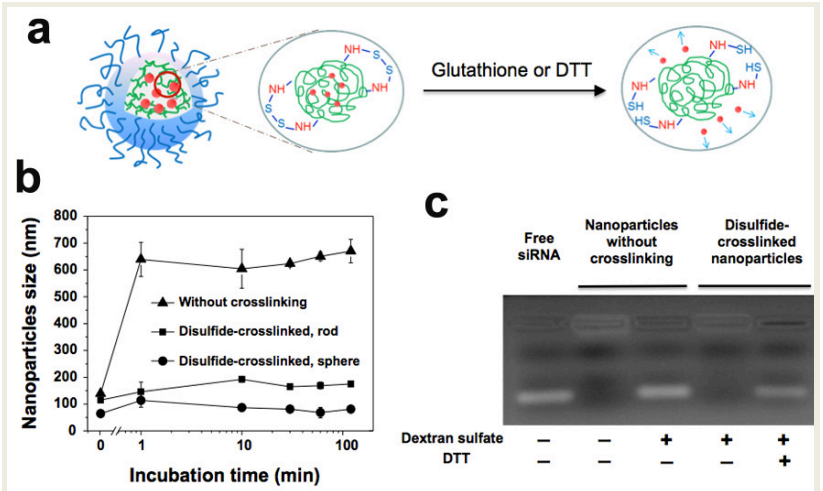

Fig. 10. Crosslinked micelles (a) remained similar sizes when treated with 10% serum (b). (c) shows the release of siRNA from disulfide-crosslinked $LPEI_{17K}$-g-PEG_{10K}/siRNA nanoparticles. Samples were incubated with DTT (50 mM) and polyanions (sodium dextran sulfate) followed by gel electrophoresis.

(GSH) inside the cytosol (Fig. 10c). These nanoparticles showed much improved stability in buffer with physiological ionic strength and bile-containing media (data not shown).

Condensed nanoparticles mediate effective gene knockdown *in vitro*. We first tested the transfection efficiency of the siRNA nanoparticles using two cell lines. This assay serves to demonstrate the bioactivity of these nanoparticles. Results showed that all three sets of nanoparticles have similar transfection efficiency in both HeLa cells and HEK293 cells (Fig. 11). It is worth noting that the micelles were less cytotoxicity in comparison with the nanoparticles prepared with LPEI/siRNA nanoparticles.

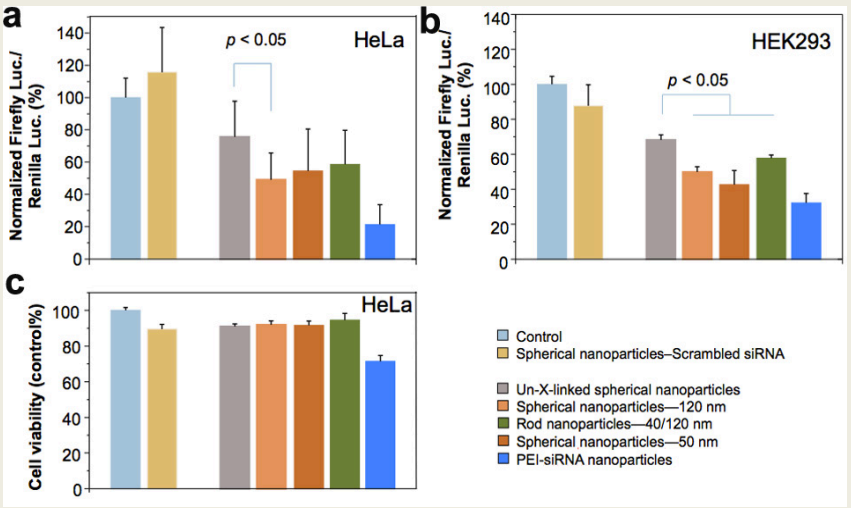

Fig. 11. *In vitro* gene silencing efficiency in Hela (***a***) and HEK293 (***b***) cells. Control groups include crosslinked $LPEI_{17K}$-g-PEG_{10K}/scrambled siRNA nanoparticles with sphere morphology and 50 nm in diameter; non-crosslinked $LPEI_{17K}$-g-PEG_{10K}/GL3 siRNA nanoparticles, and $LPEI_{17K}$/GL3 siRNA nanoparticles. Bars represent mean ± SD (n = 4).

Micellar nanoparticles mediated high knockdown efficiency *in vivo*. As a proof of principle, we first tested the gene knockdown efficiency using either intravenous injection or intrabiliary infusion as models for systematic and localized delivery systems. After local delivery "directly" to the liver hepatocytes and by-passing the first contact with Kupffer cells and serum albumin, all nanoparticle formulations showed good gene knockdown activity ranging from 50 to 80% at 2 days following infusion (Fig. 12). Among them, rod-like micellar nanoparticles, at a siRNA dose as low as 10 μg per rat, showed the highest efficiency, similar to lPEI/siRNA particles. Given the low cytotoxicity of micelles, this result is very promising.

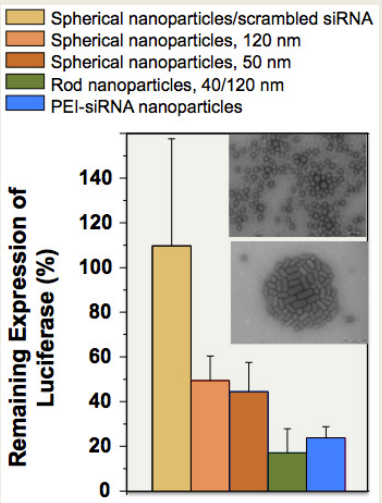

Fig. 12. Remaining luciferase expression in rat liver at 48 hours after gene knockdown treatment by retrograde intrabiliary infusion of various nanoparticle formulations. Bars represent mean ± SD (n = 4).

To further test the effect of improved stability of nanoparticles on transfection and gene knockdown efficiency, we injected nanoparticles to rats using intravenous injection at a siRNA dose of 80 μg per rat. Using the same bioluminescence imaging analysis, we have shown that the stabilized siRNA nanoparticles exhibited significantly high level of transfection and gene knockdown efficiency after systematic delivery (Fig. 13). In contrast, lPEI/siRNA were nearly ineffective. Among the micellar nanoparticles, small siRNA nanoparticles achieved nearly 80% gene knockdown at 24 h after infusion, the other two nanoparticles showed about 30 to 40% efficiency. Despite the fact that gene knockdown efficiency was recovered gradually, a more sustained knockdown effect can be

easily achieved by repeated *i.v.* injections. Although less relevant to ocular delivery, these results highlight the effectiveness of our strategy in condensing and stabilizing nanoparticles in promoting their gene knockdown activity *in vivo.*

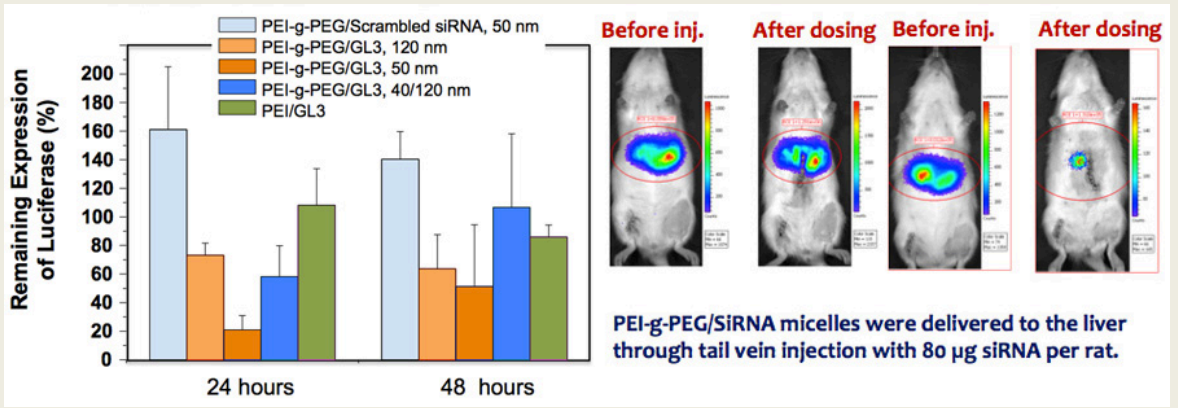

Fig. 13. Remaining luciferase expression in rat liver at 24 and 48 hours after gene knockdown treatment by intravenous injection. Bars represent mean ± SD (n = 4).

Key Research Accomplishments

We have achieved the following milestones over the past two years. To make it easier to compare, the tasks in the original proposal are list here as well.

(i). Develop chitosan/siRNA nanoparticles and PEG-PPA/siRNA nanoparticles with well characterized biophysical properties.

We have developed three sets of nanoparticles specifically designed for packaging siRNA to confer high stability, smaller size, higher size uniformity (Figs. 2, 6, and 9). These nanoparticles have been thoroughly characterized and they have been shown to be highly effective in condensing, protecting and preserving siRNA activity.

(ii). Characterize nanoparticle activities in vitro and identify the most effective nanoparticle formulation for each type of target cells.

At least two of the three nanoparticle-formulations can effectively transfect and knockdown targeted genes in human corneal epithelial cells and human corneal limbal epithelial cells (Figs. 4 and 7). The testing of the third nanoparticles in these cell type is ongoing.

(iii). Confirm delivery to target tissue and knockdown of target for ocular delivery.

Dr. Al Ruff's group has helped us testing two nanoparticle formulations (Figs. 8 and 11) through subconjunctival injection over the past six to eight months. Unfortunately, we have failed to observe detectable gene knockdown activity. We have also tested fluorescently labeled nanoparticles by this administration route. There were plentiful nanoparticles found at or near the site of injection. We are trouble-shooting this issue.

When Phase II project starts, we plan to continue to solve this problem and identify an effective nanoparticle system for ocular delivery. As soon as we observe gene knockdown activities, we will characterize the effectiveness of these nanoparticles through eye drop applications.

Reportable Outcomes

Peer-reviewed publications and manuscripts:

- Nakanishi M, Patil R, Ren Y, Shyam R, Wong P, Mao HQ. Enhanced stability and knockdown efficiency of poly(ethylene glycol)-*b*-polyphosphoramidate/siRNA micellar nanoparticles by co-condensation with sodium triphosphate. **Pharmaceutical Research.** 28(7): 1723-1732 (2011). PMID: 21387148.
- Nakanishi M, Pan D, Jiang X, Mao HQ. Hyaluronic acid-coated quaternary nanoparticles for targeted delivery of siRNA. In preparation.
- Wu J, Jiang X, Pan D, Crow MT, Mao HQ. Dual-sensitive polymer/siRNA nanoparticles with enhanced gene knockdown efficiency. In preparation.

Conference proceedings:

- Mao HQ, Jiang X, Wu J, Nakanishi M, Williford JM, Ren Y. *Engineered Nanoparticles for Gene Delivery*. Society for Biomaterials Annual Meeting, New Orleans, LA. October 6, 2012.
- Mao HQ. *Nanoparticle Engineering For Delivery of Nucleic Acid Therapeutics.* Johns Hopkins Institute for NanoBioTechnology Fifth Annual Symposium. May 4, 2012.
- Mao HQ. *Controlled Condensation of DNA and Self-Assembly of Polymer/DNA Micelles for Liver-Targeted Gene Delivery*. NIH/National Cancer Institute Seminar Series. October 13, 2011.
- Nakanishi M, Pan D, Jiang X, Mao HQ. *Stabilized quaternary nanoparticles for targeted delivery of siRNA*. The American Society of Gene and Cell Therapy 15th Annual Meeting, Philadelphia, PA. May 15–19, 2012.
- Nakanishi M, Patil R, Ren Y, Mao HQ. *Enhanced stability and knockdown efficiency of poly(ethylene glycol)-b-polyphosphoramidate/siRNA micellar nanoparticles by co-condensation with sodium triphosphate*. American Society of Gene and Cell Therapy 14th Annual Meeting, Seattle, Washington, USA, May 18-21 2011.
- Wu J, Jiang X, Pan D, Crow MT, Mao HQ. *Dual-sensitive Polymer/siRNA Nanoparticles with Enhanced Gene Knockdown Efficiency*. The 38th Annual Meeting of the Controlled Release Society. National Harbor, Washington, DC, MD, July 30-August 3, 2011.

Conclusion and Outlook

In Phase I of the Delivery System Development Core, we have successfully developed a couple of unique strategies to assemble siRNA nanoparticles through molecular design of the gene carriers, and fine-tuning of the assembly conditions. Specifically, we have developed siRNA micellar nanoparticle systems prepared from cationic copolymer carriers including poly(ethylene glycol-*b*-phosphoramidate) (PEG-*b*-PPA) copolymers, and graft copolymers of linear polyethyleneimines and polyethylene glycol (PEG). Two important approaches were developed to effectively condense siRNA to small and uniform nanoparticles (~50 nm) and to markedly enhance the colloidal and complex stability of siRNA in in physiological buffer and serum-containing media. These properties have been correlated with significantly improved siRNA delivery and gene knockdown efficiency (70–80%).

In Phase II, we plan to apply these nanoparticle systems to ocular delivery, further tailor them for transfecting corneal cell types and for improving the local tissue retention time. These optimized nanoparticles promise to delivery target siRNA more efficiently. Nanoparticle transport and delivery efficiencies in rodent models will be characterized to validate the siRNA targets and to provide guidance for nanoparticle optimization.

References

1. Nakanishi M*, et al.* (2011) Enhanced stability and knockdown efficiency of poly(ethylene glycol)-b-polyphosphoramidate/siRNA micellar nanoparticles by co-condensation with sodium triphosphate. *Pharmaceutical research* 28(7):1723-1732.
2. Sandri G*, et al.* (2004) Mucoadhesive and penetration enhancement properties of three grades of hyaluronic acid using porcine buccal and vaginal tissue, Caco-2 cell lines, and rat jejunum. *The Journal of pharmacy and pharmacology* 56(9):1083-1090.
3. Koizumi N*, et al.* (2000) Amniotic membrane as a substrate for cultivating limbal corneal epithelial cells for autologous transplantation in rabbits. *Cornea* 19(1):65-71.
4. de la Fuente M, Seijo B, & Alonso MJ (2008) Novel hyaluronic acid-chitosan nanoparticles for ocular gene therapy. *Investigative ophthalmology & visual science* 49(5):2016-2024.
5. Contreras-Ruiz L*, et al.* (2011) Intracellular trafficking of hyaluronic acid-chitosan oligomer-based nanoparticles in cultured human ocular surface cells. *Molecular vision* 17:279-290.
6. Lemarchand C, Gref R, & Couvreur P (2004) Polysaccharide-decorated nanoparticles. *European journal of pharmaceutics and biopharmaceutics : official journal of Arbeitsgemeinschaft fur Pharmazeutische Verfahrenstechnik e.V* 58(2):327-341.
7. Jiang X*, et al.* (2007) PEG-b-PPA/DNA micelles improve transgene expression in rat liver through intrabiliary infusion. *Journal of controlled release : official journal of the Controlled Release Society* 122(3):297-304.
8. Jiang X*, et al.* (2011) String-like micellar nanoparticles formed by complexation of PEG-b-PPA and plasmid DNA and their transfection efficiency. *Pharmaceutical research* 28(6):1317-1327.
9. Jiang X*, et al.* (2010) Dual-sensitive micellar nanoparticles regulate DNA unpacking and enhance gene-delivery efficiency. *Advanced materials (Deerfield Beach, Fla.)* 22(23):2556-2560.
10. Sun TM, Du JZ, Yan LF, Mao HQ, & Wang J (2008) Self-assembled biodegradable micellar nanoparticles of amphiphilic and cationic block copolymer for siRNA delivery. *Biomaterials* 29(32):4348-4355.
11. Ren Y, Jiang X, Pan D, & Mao HQ (2010) Charge density and molecular weight of polyphosphoramidate gene carrier are key parameters influencing its DNA compaction ability and transfection efficiency. *Biomacromolecules* 11(12):3432-3439.

Appendices

Published paper and selected abstracts/posters

- Nakanishi M, Patil R, Ren Y, Shyam R, Wong P, Mao HQ. Enhanced stability and knockdown efficiency of poly(ethylene glycol)-*b*-polyphosphoramidate/siRNA micellar nanoparticles by co-condensation with sodium triphosphate. **Pharmaceutical Research.** 28(7): 1723-1732 (2011). PMID: 21387148.

- Nakanishi M, Pan D, Jiang X, Mao HQ. *Stabilized quaternary nanoparticles for targeted delivery of siRNA*. The American Society of Gene and Cell Therapy 15th Annual Meeting, Philadelphia, PA. May 15–19, 2012.

- Nakanishi M, Patil R, Ren Y, Mao HQ. *Enhanced stability and knockdown efficiency of poly(ethylene glycol)-b-polyphosphoramidate/siRNA micellar nanoparticles by co-condensation with sodium triphosphate*. American Society of Gene and Cell Therapy 14th Annual Meeting, Seattle, Washington, USA, May 18-21 2011.

- Wu J, Jiang X, Pan D, Crow MT, Mao HQ. *Dual-sensitive Polymer/siRNA Nanoparticles with Enhanced Gene Knockdown Efficiency*. The 38th Annual Meeting of the Controlled Release Society. National Harbor, Washington, DC, MD, July 30-August 3, 2011.

Pharm Res
DOI 10.1007/s11095-011-0408-7

RESEARCH PAPER

Enhanced Stability and Knockdown Efficiency of Poly(ethylene glycol)-*b*-polyphosphoramidate/siRNA Micellar Nanoparticles by Co-condensation with Sodium Triphosphate

Masataka Nakanishi • Rajesh Patil • Yong Ren • Rishab Shyam • Philip Wong • Hai-Quan Mao

Received: 19 December 2010 / Accepted: 21 February 2011

ABSTRACT

Purpose Polyelectrolyte complex nanoparticles are a promising vehicle for siRNA delivery but suffer from low stability under physiological conditions. An effective stabilization method is essential for the success of polycationic nanoparticle-mediated siRNA delivery. In this study, sodium triphosphate (TPP), an ionic crosslinking agent, is used to stabilize siRNA-containing nanoparticles by co-condensation.

Methods siRNA and TPP were co-encapsulated into a block copolymer, poly(ethylene glycol)-*b*-polyphosphoramidate (PEG-*b*-PPA), to form ternary nanoparticles. Physicochemical characterization was performed by dynamic light scattering and gel electrophoresis. Gene silencing efficiency in cell lines was assessed by dual luciferase assay system.

Results The PEG-*b*-PPA/siRNA/TPP ternary nanoparticles exhibited high uniformity with smaller size (80–100 nm) compared with PEG-*b*-PPA/siRNA nanoparticles and showed increased stability in physiological ionic strength and serum-containing medium, due to the stabilization effect from ionic crosslinks between negatively charged TPP and cationic PPA segment. Transfection and gene silencing efficiency of the TPP-crosslinked nanoparticles were markedly improved over PEG-*b*-PPA/siRNA complexes in serum-containing medium. No significant difference in cell viability was observed between nanoparticles prepared with and without TPP co-condensation.

Conclusions These results demonstrated the effectiveness of TPP co-condensation in compacting polycation/siRNA nanoparticles, improving nanoparticle stability and enhancing the transfection and knockdown efficiency in serum-containing medium.

KEY WORDS block copolymer gene carrier · siRNA · sodium triphosphate · stabilization · ternary nanoparticles

INTRODUCTION

Small interfering RNA (siRNA) has been recognized as a powerful therapeutic agent for effectively silencing a specific gene on a post-transcriptional level (1–3). Many siRNA targets and RNA interference (RNAi) strategies have been devised as a therapeutic approach in the treatment of diseases such as macular degeneration, hepatitis C infection, and cancer (4,5). In spite of several recent successful reports (6), therapeutic application of siRNA has been hampered by limited stability within physiological fluids

Masataka Nakanishi and Rajesh Patil contributed equally to this work.

M. Nakanishi • R. Patil • Y. Ren • H.-Q. Mao
Department of Materials Science and Engineering
Johns Hopkins University
Baltimore, Maryland 21218, USA

M. Nakanishi • H.-Q. Mao
Translational Tissue Engineering Center, Johns Hopkins University
Baltimore, Maryland 21218, USA

R. Shyam
Department of Biomedical Engineering, Johns Hopkins University
Baltimore, Maryland 21218, USA

P. Wong
Department of Neuroscience, Johns Hopkins University
Baltimore, Maryland 21218, USA

H.-Q. Mao
Whitaker Biomedical Engineering Institute, Johns Hopkins University
Baltimore, Maryland 21218, USA

H.-Q. Mao (✉)
101E Maryland Hall, 3400 North Charles Street
Baltimore, Maryland 21218, USA
e-mail: hmao@jhu.edu

Published online: 09 March 2011

and inefficient cell membrane permeation due to high density of negative charge in naked siRNA (7,8). Therefore, development of carriers for efficient siRNA delivery has emerged as a key issue in siRNA therapeutics (9,10). Recent studies have successfully demonstrated that siRNA carriers based on various cationic polymers, lipids and peptides have been used to form nanosized polyplex with siRNA (11,12). However, these polycation/siRNA nanoparticles exhibit poor stability in buffers at physiological ionic strength or in serum-containing media due to the small molecular weight of siRNA chains (13,14). In order to improve the compaction ability and stability of siRNA-containing nanoparticles, several strategies for *in vivo* siRNA delivery have already been proposed, including siRNA conjugates with cholesterol or proteins, and the incorporation of siRNA into polymeric micelles and micro/nanogels (15,16). Huang *et al.* have shown that lipid-coated calcium phosphate nanoparticles could enhance intracellular delivery of siRNA (17). Further modifications such as cross-linking have been developed to stabilize polycation/siRNA nanoparticles in order to achieve high level of transfection. For example, Kataoka *et al.* have demonstrated increased stability of siRNA nanoparticles by cross-linking the core through disulfide bonds to increase the complex stability under physiological salt conditions (18).

We previously reported that the condensation of DNA by block copolymer, poly(ethylene glycol)-*b*-polyphosphoramidate block copolymer (PEG-*b*-PPA), yielded the self-assembled micellar nanoparticles with a complex core surrounded by a PEG corona (19,20). The advantages of these micellar nanoparticles include smaller and more uniform size, improved colloidal stability in serum-containing media, higher protection of incorporated DNA against enzymatic degradation, and prolonged blood circulation (21,22). Despite the success of mediating DNA delivery, PEG-*b*-PPA condensed micelles with siRNA suffered from low stability in salt solution, which may be due to the short and rigid structure of siRNA in contrast to plasmid DNA (13).

Here we report a new method to stabilize polycation/siRNA nanoparticles with sodium triphosphate (TPP) via ionic crosslinking (Fig. 1). TPP was first used to prepare chitosan nanoparticles by forming ionic crosslinks between positively charged amino groups of chitosan and negatively charged phosphates in TPP (23,24). TPP is popular for chitosan crosslinking because of its non-toxic nature and effective crosslinking ability (25,26). We hypothesized that similar crosslinking can form between TPP and positive-charged gene carriers, thus facilitating condensation with siRNA and increasing stability of nanoparticles. In this paper, the stability of nanoparticles with TPP-crosslinked core and the release profile of free siRNA from nanoparticle through an exchange reaction by polyanion were analyzed. Furthermore, the gene knockdown efficiency of PEG-*b*-PPA/siRNA nanoparticles stabilized by TPP was assessed in HeLa and D407 cells *in vitro*.

MATERIALS AND METHODS

Reagents

Sodium triphosphate (TPP) and poly(vinyl sulfate) potassium salt (PVSK) were purchased from Sigma-Aldrich Chemical Co. Ltd. (Milwaukee, WI, USA). WST-1 was purchased from Roche (Penzberg, Germany). UltraPure™ DNase/RNase-Free Distilled Water, Dulbecco's Modified Eagle's Medium (DMEM), Opti-MEM™ and Lipofectamine2000™ were purchased from Invitrogen (Carlsbad, CA, USA). Dual-luciferase reporter assay system and pGL3-control and pRL-CMV vectors were purchased from Promega (Madison, WI, USA). The siRNA was purchased from Ambion (Austin, TX, USA). Formvar-coated carbon grid was purchased from Electron Microscopy Sciences (Hatfield, PA, USA). The sequences of siRNA against *Photinus pyralis* luciferase were as follows: sense 5′-CUUACGCUGAGUACUUCGAdTdT-3′, antisense 5′-UCGAAGUACUCAGCGUAAGdTdT-3′.

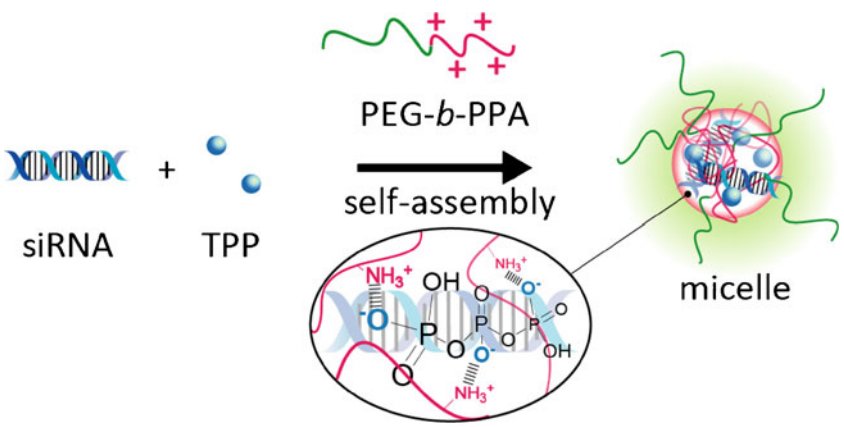

Fig. 1 Schematic of preparation of PEG-*b*-PPA/siRNA/TPP ternary micellar nanoparticles formed through ionic crosslinking with sodium triphosphate (TPP).

Preparation of Nanoparticle with TPP-Crosslinked Core

PEG-*b*-PPA (molecular weights: PEG, 12 kDa, PPA, 38 kDa) was prepared as described in the previous report (19). Ten μL of 4 μM siRNA solution (10 mM Tris–HCl, pH 7.4) was mixed with 10 μL of TPP solution (10 mM Tris–HCl, pH 7.4), followed by the addition of 20 μL of PEG-*b*-PPA solution (10 mM Tris–HCl, pH 7.4) into the mixture of siRNA and TPP solution at different mixing ratios. They were mixed by pipetting, followed by gentle vortex and spin-down. These particles were then incubated at room temperature for 1 h before use or further analysis. The mixing ratio for each formation was determined by N/P and P′/N: [primary amino group of PPA]/[phosphate group of siRNA] and [phosphate group of TPP]/[primary amino group of PPA], respectively. The negative charge number of TPP is defined as three in this study according to the report (27).

Measurement of Size and ζ-potential of Nanoparticles

Mean particle hydrodynamic diameter (*z*-average) and ζ-potential of the nanoparticles were determined by photon correlation spectroscopy and laser Doppler anemometry, respectively, using Zetasizer Nano ZS90 (Malvern Instruments, Malvern, UK) equipped with a He-Ne laser ($\lambda = 633$ nm) as the incident beam. Size distributions were determined by cumulate and histogram analysis, and results are shown as the *z*-averaged size (cumulate mean) with polydispersity index (PDI) (defined in the ISO standard document 13 321:1996). All samples were equilibrated to the defined temperature for 1 h prior to measurement. The ζ-potential values of the complexes were measured in 10 mM Tris–HCl buffer (pH 7.4) containing 150 mM NaCl at 37°C. All samples were equilibrated to the defined temperature for 1 h prior to measurement.

Stability of Nanoparticles in the Physiological Ionic Strength

The effect of crosslinking on nanoparticle stability in buffers with the physiological ionic strength was determined using the Zetasizer Nano ZS90 (Malvern Instruments). The assay was performed by measuring the size and scattering light intensity (SLI) of nanoparticles after 24 h of incubation at 37°C in solutions containing 150 mM of NaCl concentration.

Transmission Electron Microscopy

An aliquot of 10 μL of nanoparticle solution was added to a formvar carbon TEM grid and incubated for 5 min at room temperature, followed by washing with deionized water. The grid was further stained with 2% of uranyl acetate solution and washed with deoinized water twice. Transmission electron microscopy was carried out on Tecnai™ 12 (FEI Company, OR, USA) run at 100 kV.

Gel Retardation Assay

The incorporation of siRNA into nanoparticle assemblies was determined by electrophoresis on a 0.8% agarose gel. Electrophoresis was carried out at a constant voltage of 90 V for 0.5 h in TAE buffer (4.45 mM Tris-acetic acid containing 1.7 mM sodium acetate, pH 8.3). The band of migrated siRNA was visualized under a UV transilluminator (UVP, Upland, CA) at a wavelength of 365 nm after soaking the gel in distilled water containing ethidium bromide (EtBr) (0.5 μg/mL).

Stability of Encapsulated siRNA in Serum-Containing Medium

The siRNA-incorporated nanoparticles were incubated at 37°C with 50% final concentration of fetal bovine serum (FBS) for 1 and 4 h, respectively. Samples were then incubated in 10 μL of 50 mM EDTA for 5 min and 10 μL of 10 mM PVSK was added to displace siRNA from the nanoparticles. The released siRNA was analyzed by electrophoresis on a 20% polyacrylamide gel prepared in 7 M urea and TBE buffer (0.089 M Tris base, 0.089 M boric acid, and 2 mM sodium EDTA, pH 8.3). Polyacrylamide–urea gel (20%) was used due to its high efficiency in separating small fragments of possibly degraded siRNA. Electrophoresis was then carried out with 1× TBE buffer at a constant voltage of 100 V for 1 h. The siRNA bands were visualized under a UV transilluminator after staining for 40 min with a 1:10,000 dilution of SYBR-Green II RNA gel stain (Molecular Probes) in RNase-free water.

Polyanion-Exchange Analysis

Self-assembled nanoparticles prepared above were incubated with in 10 mM Tris–HCl, pH 7.4 at [sulfonate of PVSK]/[phosphate of siRNA] ratio of 5 at 37°C for 5 h. The released siRNA from nanoparticles was analyzed at 1 and 5 h by the gel retardation assay under the same conditions as described above.

Knockdown Efficiency by Nanoparticles and Cell Viability

HeLa cells (human epithelial cervical cancer cell line) and D407 cells (human retinal pigment epithelial cell line) were seeded onto 24-well culture plates at a density of 5×10^4 cells per well in 500 μL of medium, followed by 20 h of

incubation in DMEM containing 10% fetal bovine serum (FBS) without antibiotics. Then, 720 ng/well pGL3-control plasmid encoding *Photinus pyralis* luciferase (P-Luc) and 80 ng/well pRL-CMV plasmid encoding *Renilla reniformis* luciferase (R-Luc) were co-transfected to the cells with Lipofectamine2000™ according to the manufacturer's instructions; cells were further incubated for 4 h. For nanoparticle-transfection groups, the medium was replaced with fresh serum-free medium or medium with 10% FBS, and nanoparticles containing siRNA (100 nM) against P-Luc with or without TPP crosslinking were applied to each well and incubated for 4 h. The medium was then replaced with complete media containing 10% serum, followed by incubation at 37°C with a 5% of CO_2atm. After 44 h, cells were rinsed with PBS and subjected to a luciferase expression assay using the Dual-Luciferase Reporter Assay System. For each assay, P-Luc and R-Luc luminescence was measured using FLUOstar OPTIMA plate reader (BMG LABTECH, Germany) after the addition of appropriate substrates. P-Luc activities were normalized by R-Luc activities, and values are expressed as a ratio to the control value (mean ± SD, $n=4$). Cell viability was determined using WST-1 according to the manufacture's protocol. Incubation conditions were identical to those used in the transfection protocol.

RESULTS

Preparation of PEG-*b*-PPA/siRNA Nanoparticles and Stabilization with TPP

In order to test whether TPP co-condensation enhances the nanoparticle formation, we prepared PEG-*b*-PPA/siRNA nanoparticles with TPP added to the siRNA solution. PEG-*b*-PPA solutions were incubated with a mixture of siRNA and TPP at N/P ratios of 4 and 8 and a variety of P′/N ratios of 0 to 1 to form polyelectrolyte complexes (Fig. 2). In the absence of TPP (P′/N=0), there is no distinct particle formation for N/P ratios of both 4 and 8, where the measured *z*-average size was less than 10 nm with large PDI (Fig. 2a and b). On the other hand, when TPP was used during the condensation, nanoparticle formation was observed at P′/N ratio of 0.1 or higher. The mean particle size of the assembled nanoparticles with TPP-co-condensation increased to 80 to 100 nm as measured by DLS (Fig. 2a and b). Of interest, PDI of nanoparticles prepared with TPP was less than 0.1, and the histogram analysis showed unimodal size distribution. These data indicated that TPP was highly effective in facilitating siRNA condensation and nanoparticle formation.

Significant differences in particle morphology were also observed in transmission electron microscopy (TEM) analysis between nanoparticle preparations in the presence and absence of TPP. TEM images of nanoparticles prepared with TPP showed that these particles were mostly spherical with diameters ranging from 80 to 100 nm (Fig. 2c), corroborating well with the average size (98.2± 10.2 nm) measured by DLS method. On the other hand, the TEM images of particles formed without TPP revealed aggregates with irregular shape and sized ranged from 20 to 100 nm, correlating with higher PDI. Nanoparticles with TPP showed much higher contrast than that without TPP in TEM images, indicating that the TPP-condensed nanoparticles may have more compact polyplex core than that without TPP.

As shown in Fig. 2d, the ζ-potential values of nanoparticles prepared at different P′/N ratios varied significantly and appeared to be highly dependent on P/N ratio. The ζ-potential values decreased sharply from +15 to −1.5 mV when the P′/N ratio increased from 0.1 to 1.0. The near electrostatic neutrality of the particle surface at P′/N ratio of 0.5 to 1.0, with a PEG corona, may be advantageous in preventing nanoparticle aggregation when applied in physiological media.

Complex Stability of Nanoparticles in Salt Solution with Physiological Ionic Strength

The complex stability of nanoparticles was assessed by monitoring changes in size and PDI in 0.15 M of NaCl solution. No dynamic scattering signals were detected for nanoparticles prepared without TPP (P′/N=0) at N/P ratio of 4 or 8 after they were incubated with 0.15 M NaCl solution, due to the charge screening effect. Nanoparticles prepared with lower P′/N ratios (0.1 and 0.2) showed increased sizes after incubating in 0.15 M NaCl. In contrast, nanoparticles prepared at higher P′/N ratios only showed slightly increased particle sizes (average size of 110 and 100 nm for N/P of 4 and 8, respectively) and low PDIs (Fig. 2a and b). This indicates that TPP-crosslinked nanoparticles could stabilize siRNA nanoparticles in a solution with physiological ionic strength.

Nanoparticle Stability in the Presence of 50% Bovine Serum

To test whether the encapsulated siRNA showed improved stability in serum containing medium, nanoparticles were incubated with 50% of fetal bovine serum (FBS) at 37°C followed by gel electrophoresis to analyze the integrity of siRNA. Figure 3 showed that siRNA incubated with 50% FBS was significantly degraded. On the other hand, siRNA recovered from nanoparticles only showed trace amount of degradation for all N/P and P′/N ratios. The siRNA recovered from nanoparticles with and without TPP were

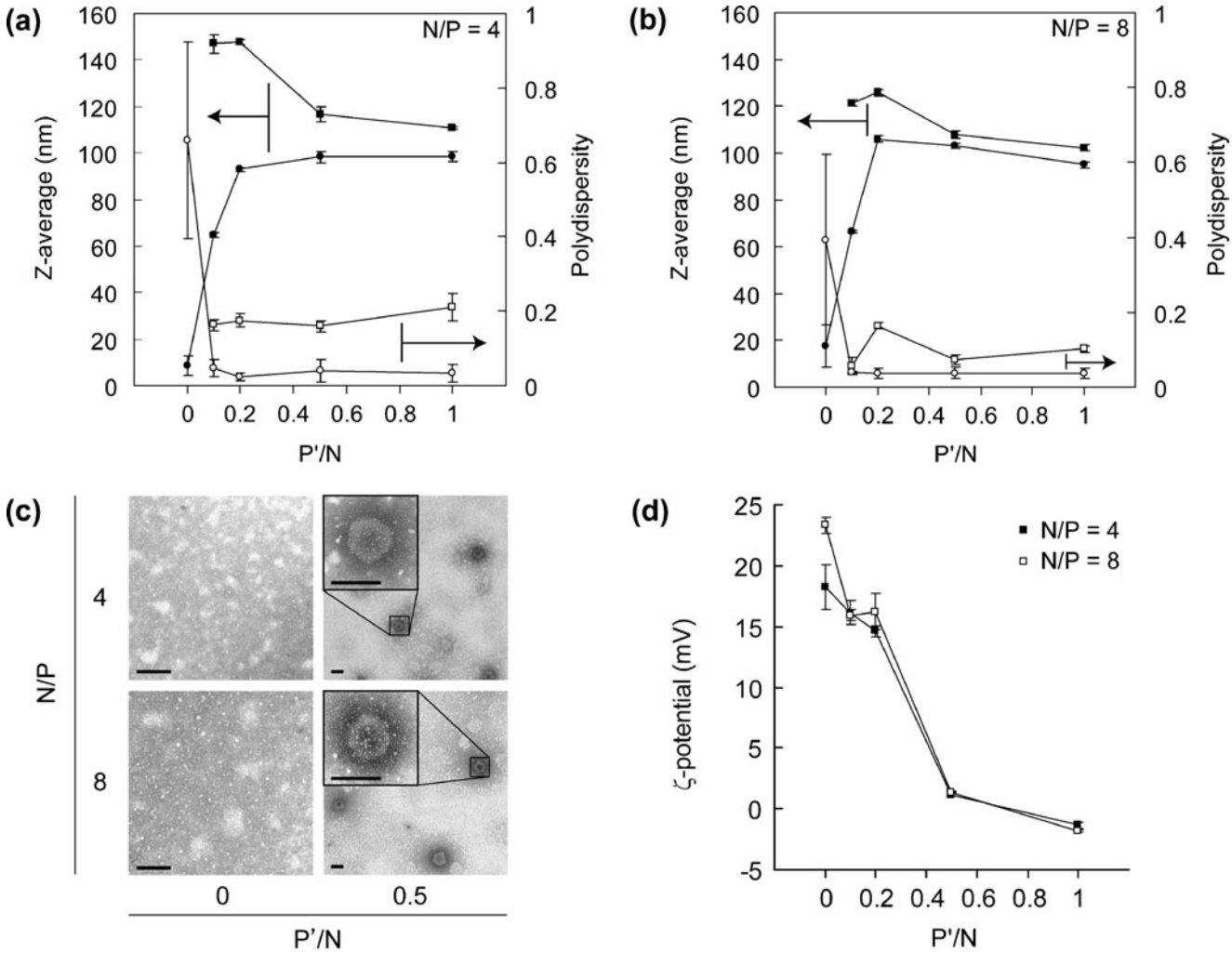

Fig. 2 The *z*-average (*left ordinate*) and PDI (*right ordinate*) measured by dynamic light scattering analysis of nanoparticles formed at various P′/N ratios and N/P ratios of 4 (**a**) and 8 (**b**), respectively, before (*filled circle*, *empty circle*) and after (*filled square*, *empty square*) incubation with 150 mM NaCl for 24 h. Values represent Mean ± SEM ($n = 3$). Particles without TPP crosslinking dissociated after incubation in 150 mM NaCl; therefore, no data points were included for P′/N = 0 for salt incubation lines (*filled square*, *empty square*) here. (**c**) TEM images of nanoparticle formed at P′/N ratios of 0 and 0.5 for N/P ratios of 4 and 8, respectively. Scale bar = 100 nm. (**d**) Zeta-potential of nanoparticles prepared at various P′/N ratios for N/P ratios of 4 (*filled square*) and 8 (*empty square*), respectively. Values represent Mean ± SEM ($n = 3$).

still more intact for 4 h at all the P′/N ratios. No significant difference on siRNA integrity in 50% FBS was observed between nanoparticles prepared with and without TPP. PEG-*b*-PPA/siRNA nanoparticles without TPP showed similar resistance of siRNA to enzymatic degradation for 4 h of incubation with 50% serum as compared to nanoparticles with TPP.

Complex Stability of Nanoparticles Against Challenges with Polyanions

The encapsulation efficiency of siRNA into nanoparticles was confirmed by agarose gel electrophoresis (Fig. 4a and d). Free siRNA was not observed for all samples including the complexes prepared with or without TPP, highlighting the good siRNA condensation ability of PEG-*b*-PPA. More importantly, the complexation ability was not compromised by the addition of TPP at all P′/N ratios tested. In combining with the DLS analysis (Fig. 2a and b), these data indicated that complexation between PEG-*b*-PPA and siRNA was strong enough to inhibit the gel migration ability of siRNA at both N/P ratios of 4 and 8, but distinct particle formation was observed only with TPP-assisted condensation.

The stability of the nanoparticles was also analyzed by characterizing the release profile of incorporated siRNA using a polyanion-exchange reaction (Fig. 4b, c, e, and f) (28,29). There exist various types of anionic polymers, including anionic proteins, sulfated polysaccharides, nuclear chromatin and messenger RNA (mRNA), as essential

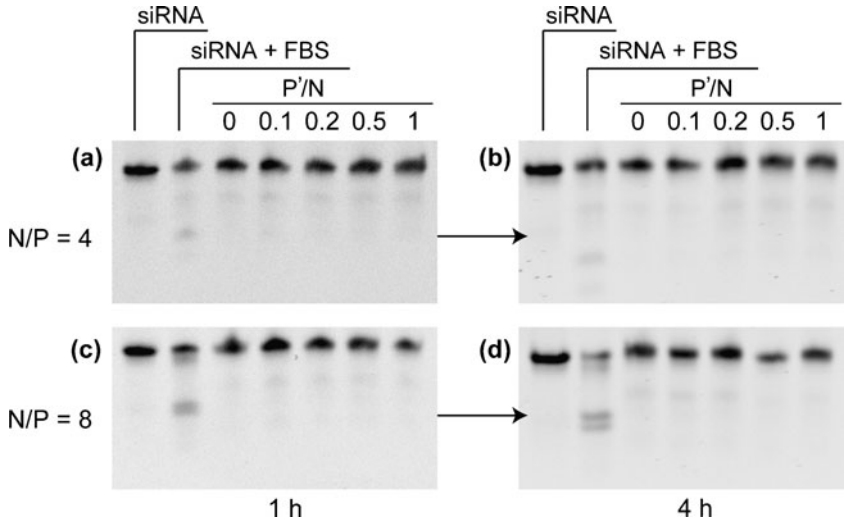

Fig. 3 Gel retardation assay of siRNA integrity in nanoparticles against enzymatic degradation in 50% FBS. Nanoparticles prepared at various conditions were incubated in 50% FBS for 1 h (**a** and **c**) and 4 h (**b** and **d**), respectively.

cellular components. Exchange reaction of polycations with these negatively charged polymers may take place in biological environment. As a result, siRNA may be released from nanoparticles through the intermolecular exchange and facilitate a series of subsequent RNAi processes for gene silencing. On the other hand, nanoparticles should be sufficiently stable to resist decomplexation and release of siRNA before they reach the cytosol of target cells. Therefore, maintaining a balanced complex stability is important to successful transfection and subsequent knockdown of the desired target.

Figure 4 showed that nanoparticle stability increased with increasing P′/N ratio and N/P ratio. Incubation of nanoparticle with PVSK for 1 h resulted in minimal release of siRNA from particles formed with N/P ratios of 4 and 8 at various P′/N ratios. However, the differences began to emerge at a later time point (5 h after incubation). The intensity of released siRNA bands were easily detected, and their intensity decreased with increasing P′/N ratio. Moreover, the observed intensity of migratory siRNA band at N/P of 8 was slightly weaker than that at N/P of 4. These data gave comparative stabilities of various nanoparticles prepared with different N/P and P′/N ratios, confirming that both PEG-b-PPA and TPP contributed to the stability of nanoparticles.

Transfection and Knockdown Efficiency of PPA-*b*-PPA/siRNA Nanoparticles

The knockdown efficiency of PPA-*b*-PPA/siRNA nanoparticles *in vitro* was assessed in two different types of cells, human epithelial cervical cancer cells (HeLa) and human

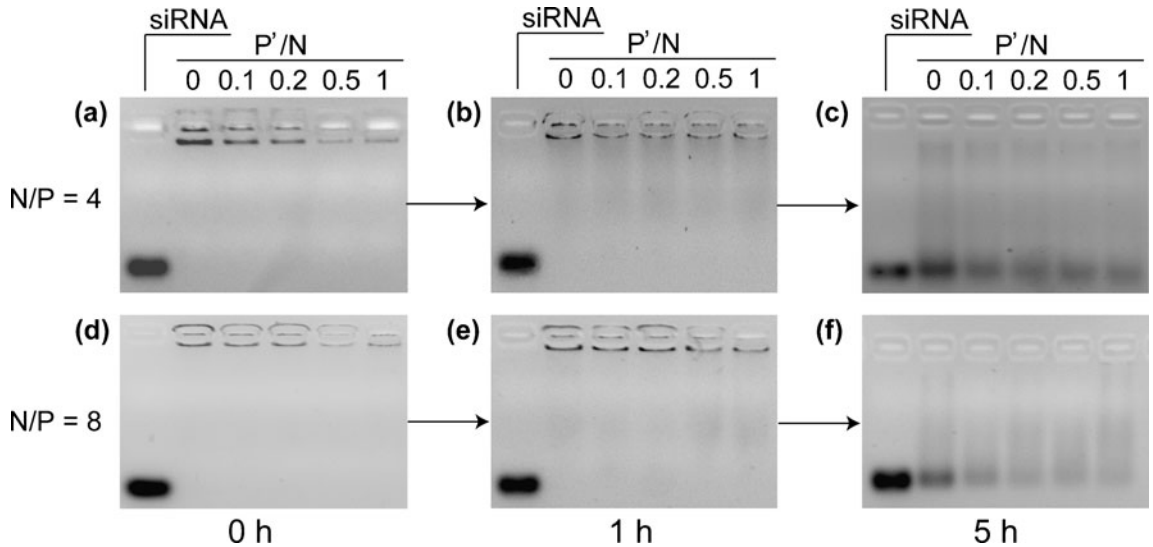

Fig. 4 Gel retardation assay of complexation efficiency for siRNA at various P′/N ratios for N/P ratios of 4 and 8, respectively. Nanoparticles prepared at various conditions were incubated with PVSK for 1 and 5 h at 37°C at a molar ratio of sulfate groups in PVSK to phosphate groups in siRNA of 5.

retinal pigment epithelial cells (D407) in the absence (Fig. 5a) and presence of serum (Fig. 5b). In this experiment, HeLa and D407 cells were transiently transfected respectively with the two kinds of reporter genes P-Luc and R-Luc, followed by the treatment with nanoparticles prepared at different P′/N ratios (0 to 1.0) with siRNA against P-Luc. The expression level of R-Luc was used as an internal reference for the initial transgene expression level. After transfection period of 44 h, the inhibition of P-Luc expression was evaluated by measuring the relative expression ratio of P-Luc/R-Luc at a concentration of 100 nM siRNA.

Although PEG-*b*-PPA/siRNA complexes without TPP failed to show distinct measurement of nanoparticles in DLS, they mediated an average of 24% and 58% knockdown efficiency in HeLa cells and 40% to 56% in D407 cells in serum-free medium at N/P ratios of 4 and 8, respectively. TPP-crosslinked nanoparticles resulted in higher knockdown efficiencies at both N/P ratios in both cell lines. As the P′/N ratio increases, the gene knockdown efficiency increased gradually. At N/P ratio of 4, the knockdown efficiency reached the plateau of ca. 60% at P′/N ratio of 0.5 in HeLa cells and the highest knockdown efficiency of ca. 60% at P′/N ratio of 1.0 in D407 cells (Fig. 5a). The knockdown efficiency was higher at N/P of 8 and reached ca. 75% of knockdown efficiency in both types of cells.

Interestingly, however, when the transfections were conducted in 10% serum-containing medium, the knockdown efficiency of PEG-*b*-PPA/siRNA complexes without TPP stabilization was significantly reduced compared to that obtained in serum-free condition (Fig. 5b). The knockdown efficiency for N/P ratio of 4 was 10–12%, and 23–34% at N/P ratio of 8 in both cell lines. In contrast, the knockdown efficiency of TPP-crosslinked nanoparticles was maintained or slightly enhanced as compared to that obtained in serum-free medium transfection. As the P′/N ratio increased, the gene knockdown efficiency maintained a similar level in HeLa cells and moderately increased in D407 cells. At N/P ratio of 4, the knockdown efficiency reached the plateau of ca. 50% in Hela cells and a maximum of 70% in D407 cells. Higher knockdown efficiency was obtained at N/P of 8 for both cell lines, with 75% to 80% knockdown efficiency obtained in HeLa cells and D407 cells, respectively, at P′/N ratio of 1.

Cytotoxicity of PEG-*b*-PPA/siRNA Nanoparticles

The potential cytotoxicity of PEG-*b*-PPA/siRNA nanoparticles was assessed in HeLa cells and D407 cells under the transfection conditions. The cell viability was determined by WST assay using water-soluble tetrazolium salt (Fig. 6). Nearly 100% of cell viability was observed for all transfection conditions in HeLa cells, and over 90% of cell viability of D407 cells was observed under the same conditions. There was no significant difference in cell viability observed between nanoparticles prepared with and without TPP crosslinking. Similar cytotoxicity results were obtained under serum-free transfection condition (data not shown). These results demonstrated that the addition of TPP into nanoparticle assemblies did not influence their cytotoxicity.

DISCUSSION

Compacting siRNA with polymeric carrier into distinct, small and stable nanoparticles has been challenging due to the much lower molecular weight and condensation ability of siRNA as compared with plasmid DNA. Particle size and size distribution are important determinants for successful

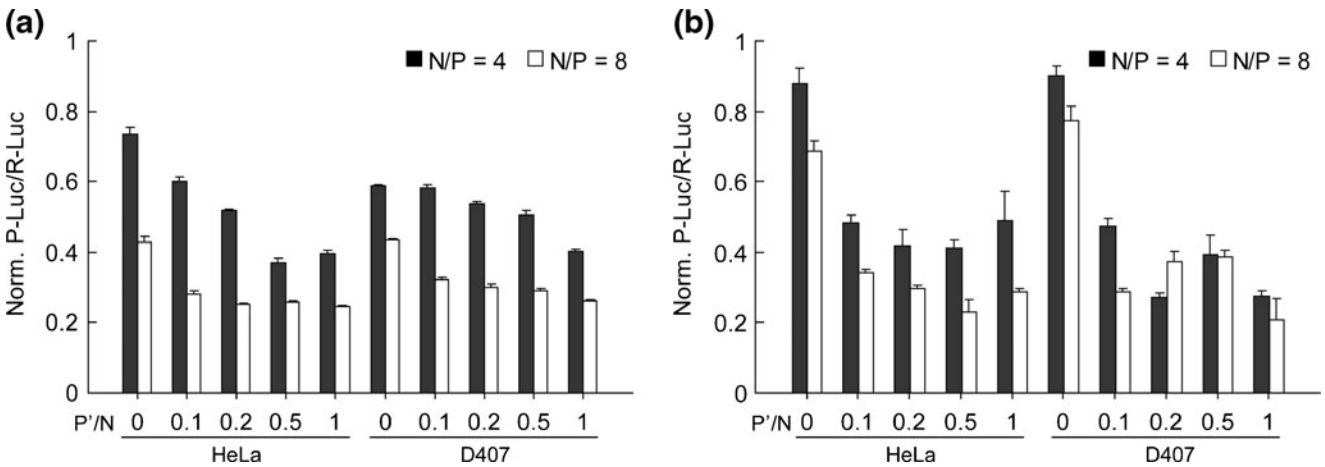

Fig. 5 Gene silencing efficiency mediated by PEG-PPA/siRNA/TPP ternary nanoparticles at various P′/N ratios for N/P ratios of 4 and 8 in HeLa and D407 cells in the absence (**a**) and presence (**b**) of 10% serum. A siRNA dose of 100 nM was used in all transfection groups. Values are expressed as Mean ± SEM ($n = 4$).

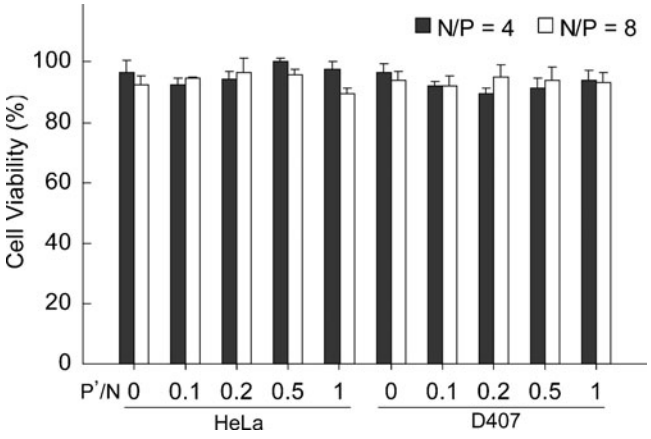

Fig. 6 Viability of HeLa and D407 cells transfected with PEG-PPA/siRNA/TPP ternary nanoparticles in 10% serum-containing medium under the conditions described in Fig 5. Values are expressed as Mean ± SEM ($n = 4$).

gene transfection and transport properties *in vivo*. It has been reported that particles in the nanometer-sized range have a relatively higher cellular uptake and intracellular transport compared to microsized particles (30–33). Here we proposed a convenient method to enhance the condensation between PEG-*b*-PPA and siRNA. Smaller and more uniform nanoparticles were formed with relatively low concentration of TPP at lower N/P ratios. The major advantages of TPP as a stabilization crosslinker are its low toxicity and the convenience of simply mixing TPP and siRNA solution before complexing with PEG-*b*-PPA. In addition, the inclusion of TPP did not interfere with the complexation between PEG-*b*-PPA and siRNA.

Although PEG-*b*-PPA and siRNA formed complexes at N/P ratios of 4 and 8, particles were irregularly shaped with wide size distribution. The addition of TPP drastically improved the condensation efficiency, forming spherical nanoparticles with small and distinct sizes at P′/N ratio as low as 0.2. The mechanism of enhanced condensation is likely through intermolecular electrostatic interaction, due to the multivalent anionic nature of TPP. Mixing PEG-*b*-PPA with TPP only (without siRNA) at a P′/N ratio between 0.1 and 1.0 also formed particles with average size ranging from 180 to 200 nm and a PDI of ca. 0.3 (data not shown). This confirms that TPP has the ability to condense polycations and form nanoparticles through electrostatic interaction. These particles exhibited much bigger size and PDI as compared with PEG-*b*-PPA/siRNA/TPP nanoparticles. Together with the observation of unimodal distribution of PEG-*b*-PPA/siRNA/TPP nanoparticles, these results indirectly confirmed that TPP participated in forming the ternary nanoparticles, rather than forming separate populations of PEG-*b*-PPA/TPP and PEG-*b*-PPA/siRNA particles.

Another advantage of the PEG-*b*-PPA/siRNA/TPP nanoparticle system is the tunable stability. The complex stability of the ternary nanoparticles was found to be dependent on N/P and P′/N ratios. The stabilization effect of TPP increased with P′/N ratio and was more pronounced at lower N/P ratio. In general, the PEG-*b*-PPA/siRNA/TPP ternary nanoparticles were smaller and more stable at higher N/P and P′/N ratios. Based on the required stability for different gene knockdown applications, it may be possible to fine-tune the stability of the ternary nanoparticles to maintain sufficient stability for nanoparticles to transport to target cells, escape endolysosomal compartment, reach the cytosol of target cells, and allow intracellular release of siRNA in physiological ionic strength and in the presence of polyelectrolytes. On the other hand, siRNA integrity in serum condition was less dependent on all N/P and P′/N ratios tested. Resistance of siRNA to enzymatic degradation is not the major reason for enhanced knockdown efficiency, because complexes formed without TPP crosslinking showed similar protection to siRNA in 50% FBS-containing medium. This result was similar to that reported in the case of PEG-*b*-polylysine/siRNA complexes (18).

The co-condensation of TPP also significantly modulated the nanoparticle surface charge. The ζ-potential of the ternary nanoparticles reduced drastically to neural at a P′/N ratio of 0.5. This may significantly impact the *in vivo* nanoparticle transport and stability, as positively charged nanoparticles are prone to opsinization and passive adsorption with abundant negatively charged serum proteins, leading to particle aggregation and uptake by macrophages. This hypothesis remains to be tested in an *in-vivo* transfection study in the near future.

The improved stability of the ternary nanoparticle systems correlated well with their enhanced gene knockdown efficiency over PEG-*b*-PPA/siRNA complexes. Although the enhancement effect was less pronounced at higher N/P ratio, the TPP-crosslinked nanoparticles showed the highest transfection and transgene knockdown efficiency for all P′/N and N/P ratios tested. More importantly, the knockdown efficiency of PEG-*b*-PPA/siRNA complexes in serum-containing medium was significantly reduced as compared to that obtained in serum-free transfection in both cell lines, whereas the efficiency was maintained or enhanced for TPP-crosslinked nanoparticles in serum-containing medium in both cell lines and at both N/P ratios. Given that TPP-crosslinked nanoparticles at higher P′/N ratios showed neutral or negative surface charges, which likely decreased nanoparticle binding with cell surface, hence reducing cellular uptake, the higher knockdown efficiency of ternary nanoparticles may primarily be attributed by the more compact size and increased complex stability of nanoparticles. Both factors may favor particle uptake and the protection of siRNA during endocytosis and in endolysosomal compartment, eventually leading to improved gene knockdown activity. More

detailed mechanistic understanding of the intracellular trafficking TPP-crosslinked nanoparticles as a function of P′/N ratio remains to be investigated.

Finally, this stabilization strategy for PEG-*b*-PPA/siRNA complexes has minimal side effect, as the cytotoxicity profile of the ternary nanoparticles was the same as PEG-*b*-PPA/siRNA complexes without TPP addition. This is consistent with the low toxicity profile of TPP, which is an FDA direct food additive (21 CFR 173.310) and is on the GRAS (generally recognized as safe) list.

CONCLUSIONS

In this study, we demonstrated that co-condensation with TPP was a safe and effective approach to improve the complex stability and gene silencing efficiency of PEG-*b*-PPA/siRNA nanoparticles. By simply mixing TPP with siRNA before condensing with PEG-*b*-PPA, spherical ternary nanoparticles with smaller size and narrow distribution were obtained. These ternary nanoparticles showed improved complex stability in salt and serum-containing medium and against polyanion exchange reaction. The stability of ternary nanoparticles increased with increasing P′/N and N/P ratios. The release of encapsulated siRNA was observed following incubation with polyanions. The improved stability correlated well with the enhanced transfection and gene knockdown efficiency of the ternary nanoparticles. The knockdown efficiency of TPP-crosslinked nanoparticles was much higher than PEG-*b*-PPA/siRNA complexes in serum-containing medium. These results highlight the TPP-co-condensation as a promising strategy to improve the efficiency of polymer/siRNA nanoparticle-mediated gene knockdown approaches.

ACKNOWLEDGMENTS

The authors thank Dr. James F. Dillman III and Dr. Albert L. Ruff at the Cell and Molecular Biology Branch, US Army Medical Research Institute of Chemical Defense, and Dr. Xuan Jiang at Department of Materials Science and Engineering, Johns Hopkins University, for discussions throughout the study. We thank Dr. Noriko Esumi for providing D407 cells. This study was supported by US Army Defense Threat Reduction Agency through the Grant W81XWH-10-2-0053.

REFERENCES

1. Kim DH, Behlke MA, Rose SD, Chang MS, Choi S, Rossi JJ. Synthetic dsRNA Dicer substrates enhance RNAi potency and efficacy. Nat Biotechnol. 2005;23:222–6.
2. Elbashir SM, Lendeckel W, Tuschl T. RNA interference is mediated by 21-and 22-nucleotide RNAs. Genes Dev. 2001;15:188–200.
3. Elbashir SM, Harborth J, Lendeckel W, Yalcin A, Weber K, Tuschl T. Duplexes of 21-nucleotide RNAs mediate RNA interference in cultured mammalian cells. Nature. 2001;411:494–8.
4. Grimmand D, Kay MA. Therapeutic application of RNAi: is mRNA targeting finally ready for prime time? J Clin Investig. 2007;117:3633–41.
5. Manoharan M. RNA interference and chemically modified small interfering RNAs. Curr Opin Chem Biol. 2004;8:570–9.
6. Guo PX, Coban O, Snead NM, Trebley J, Hoeprich S, Guo SC, *et al*. Engineering RNA for targeted siRNA delivery and medical application. Adv Drug Deliv Rev. 2010;62:650–66.
7. Nothisen M, Kotera M, Voirin E, Remy JS, Behr JP. Cationic siRNAs provide carrier-free gene silencing in animal cells. J Am Chem Soc. 2009;131:17730–1.
8. Eguchiand A, Dowdy SF. siRNA delivery using peptide transduction domains. Trends Pharmacol Sci. 2009;30:341–5.
9. Frohlichand T, Wagner E. Peptide- and polymer-based delivery of therapeutic RNA. Soft Matter. 2010;6:226–34.
10. David S, Pitard B, Benoit JP, Passirani C. Non-viral nanosystems for systemic siRNA delivery. Pharmacol Res. 2010;62:100–14.
11. Jeong JH, Kim SW, Park TG. Molecular design of functional polymers for gene therapy. Prog Polym Sci. 2007;32:1239–74.
12. Khurana B, Goyal AK, Budhiraja A, Arora D, Vyas SP. siRNA delivery using nanocarriers—an efficient tool for gene silencing. Curr Gene Ther. 2010;10:139–55.
13. Mok H, Lee SH, Park JW, Park TG. Multimeric small interfering ribonucleic acid for highly efficient sequence-specific gene silencing. Nat Mater. 2010;9:272–8.
14. Bolcato-Bellemin AL, Bonnet ME, Creusatt G, Erbacher P, Behr JP. Sticky overhangs enhance siRNA-mediated gene silencing. Proc Natl Acad Sci USA. 2007;104:16050–5.
15. Raemdonck K, Van Thienen TG, Vandenbroucke RE, Sanders NN, Demeester J, De Smedt SC. Dextran microgels for time-controlled delivery of siRNA. Adv Funct Mater. 2008;18:993–1001.
16. Tamura A, Oishi M, Nagasaki Y. Enhanced cytoplasmic delivery of siRNA using a stabilized polyion complex based on PEGylated nanogels with a cross-linked polyamine structure. Biomacromolecules. 2009;10:1818–27.
17. Li J, Chen YC, Tseng YC, Mozumdar S, Huang L. Biodegradable calcium phosphate nanoparticle with lipid coating for systemic siRNA delivery. J Control Release. 2010;142:416–21.
18. Matsumoto S, Christie RJ, Nishiyama N, Miyata K, Ishii A, Oba M, *et al*. Environment-responsive block copolymer micelles with a disulfide cross-linked core for enhanced siRNA delivery. Biomacromolecules. 2009;10:119–27.
19. Jiang X, Dai H, Ke CY, Mo X, Torbenson MS, Li ZP, *et al*. PEG-b-PPA/DNA micelles improve transgene expression in rat liver through intrabiliary infusion. J Control Release. 2007;122:297–304.
20. Jiang X, Zheng Y, Chen HH, Leong KW, Wang TH, Mao HQ. Dual-sensitive micellar nanoparticles regulate DNA unpacking and enhance gene-delivery efficiency. Adv Mater. 22:2556–60.
21. Allen TM, Hansen C, Martin F, Redemann C, Yauyoung A. Liposomes containing synthetic lipid derivatives of poly(ethylene glycol) show prolonged circulation half-lives *inviv*o. Biochim Biophys Acta. 1991;1066:29–36.
22. Klibanov AL, Maruyama K, Torchilin VP, Huang L. Amphipathic polyethyleneglycols effectively prolong the circulation time of liposomes. FEBS Lett. 1990;268:235–7.
23. Calvo P, RemunanLopez C, VilaJato JL, Alonso MJ. Chitosan and chitosan ethylene oxide propylene oxide block copolymer

nanoparticles as novel carriers for proteins and vaccines. Pharm Res. 1997;14:1431–6.
24. Calvo P, RemunanLopez C, VilaJato JL, Alonso MJ. Novel hydrophilic chitosan-polyethylene oxide nanoparticles as protein carriers. J Appl Polym Sci. 1997;63:125–32.
25. Park JH, Saravanakumar G, Kim K, Kwon IC. Targeted delivery of low molecular drugs using chitosan and its derivatives. Adv Drug Deliv Rev. 2010;62:28–41.
26. Mao SR, Sun W, Kissel T. Chitosan-based formulations for delivery of DNA and siRNA. Adv Drug Deliv Rev. 2010;62:12–27.
27. Nasti A, Zaki NM, de Leonardis P, Ungphaiboon S, Sansongsak P, Rimoli MG, *et al.* Chitosan/TPP and chitosan/TPP-hyaluronic acid nanoparticles: systematic optimisation of the preparative process and preliminary biological evaluation. Pharm Res. 2009;26:1918–30.
28. Bakeev KN, Izumrudov VA, Kuchanov SI, Zezin AB, Kabanov VA. Kinetics and mechanism of interpolyelectrolyte exchange and addition-reactions. Macromolecules. 1992;25:4249–54.
29. Katayoseand S, Kataoka K. Water-soluble polyion complex associates of DNA and poly(ethylene glycol)-poly(L-lysine) block copolymer. Bioconjug Chem. 1997;8:702–7.
30. Ishida O, Maruyama K, Tanahashi H, Iwatsuru M, Sasaki K, Eriguchi M, *et al.* Liposomes bearing polyethyleneglycol-coupled transferrin with intracellular targeting property to the solid tumors *in vivo*. Pharm Res. 2001;18:1042–8.
31. Litzinger DC, Buiting AMJ, Vanrooijen N, Huang L. Effect of liposome size on the circulation time and intraorgan distribution of amphipathic poly(ethylene glycol)-containing liposomes. Biochim Biophys Acta, Biomembr. 1994;1190:99–107.
32. Uchiyama K, Nagayasu A, Yamagiwa Y, Nishida T, Harashima H, Kiwada H. Effects of the size and fluidity of liposomes on their accumulation in tumors—a presumption of their interaction with tumors. Int J Pharm. 1995;121:195–203.
33. Akitaand H, Harashima H. Advances in non-viral gene delivery: using multifunctional envelope-type nano-device. Expert Opin Drug Deliv. 2008;5:847–59.

The 38th Annual Meeting of the Controlled Release Society. National Harbor, Washington, DC, MD, July 30-August 3, 2011.

Dual-sensitive Polymer/siRNA Nanoparticles with Enhanced Gene Knockdown Efficiency

Juan Wu[1], Xuan Jiang[1], Deng Pan[1], Michael T. Crow[2] and Hai-Quan Mao[*,1,3]
[1]Department of Materials Science and Engineering, Whitaker Biomedical Engineering Institute, Johns Hopkins University
[2]Department of Medicine, Division of Pulmonary and Critical Care Medicine, [3]Translational Tissue Engineering Center, Johns Hopkins School of Medicine, Baltimore, Maryland, USA
Email: juanwu@jhu.edu

ABSTRACT SUMMARY

Dual-sensitive siRNA nanoparticles based on linear polyethylenimine-graft-poly(ethylene glycol) copolymer (LPEI-*g*-PEG) is used for cytoplasmic siRNA delivery. This graft copolymer could condense siRNA into uniform LPEI-*g*-PEG/siRNA nanoparticles, which were further stabilized by reversible disulfide crosslinks. Delivery of GFP-22 siRNA with these dual-sensitive nanoparticles significantly inhibited the endogenous GFP expression in rat distal pulmonary artery smooth muscle cells (PASMCs) compared with non-crosslinked LPEI-*g*-PEG/siRNA nanoparticles.

INTRODUCTION

Polymer-based gene carriers have been increasingly proposed as a safer alternative to viral vectors, due to their advantages on low immune response and cytoxicity, high versatility in modulating nanoparticle properties and delivery profile, and the ease of large scale production.[1] Linear polyethylenimine (LPEI) is one of the most efficient and widely studied synthetic carriers for the delivery of plasmid DNA or siRNA into cells *in vitro* and *in vivo*.[2] However, siRNA-containing polyplexes prepared with high molecular weight LPEI mediate higher knockdown efficiency, but show relatively high toxicity. Another major challenge for LPEI/siRNA nanoparticles *in vivo* is their poor colloidal stability and serum stability, which lead to rapid aggregation followed by macrophage uptake and the premature dissociation of nanoparticles and release of siRNA payload.

Here, we present a novel dual-sensitive siRNA nanoparticle system based on LPEI-*g*-PEG copolymer for siRNA delivery. In order to decrease cytotoxicity and improve the colloidal stability of these nanoparticles in aqueous solution, LPEI was conjugated with hydrophilic and biocompatible poly(ethylene glycol). We then introduced reversible reduction-sensitive crosslinking to stabilize LPEI-*g*-PEG/siRNA nanoparticles. The resulting disulfide-crosslinked LPEI-*g*-PEG nanoparticles showed dual-sensitivity that offer higher stability in serum and endolysosomal compartment, upon reduction of disulfide crosslinks in cytosol, the nanoparticles will became unstable in physiological ionic strength and hence facilitate the release of the siRNA cargo inside the cytosol.

EXPERIMENTAL METHODS

Synthesis of LPEI-*g*-PEG copolymer. Poly-ethylene glycol succinimidyl succinate (M_W =10 KDa) was conjugated to LPEI (M_W = 17 KDa). Briefly, LPEI (4 mg) was dissolved in 10 mL of 2-(4-morpholino) ethanesulfonic acid buffer (MES buffer, 0.1 M, pH 6.5), to which was added polyethylene glycol succinimidyl succinate (40 mg) in 40 mL of MES buffer. The reaction was performed at room temperature for 24 h. The product was purified by dialysis against DI water (MWCO 12 – 14 KDa) for 1 day to remove the unreacted PEG, and then, the purified product was harvested by freeze-drying.

Preparation of polycations/siRNA nanoparticles. GFP-22 siRNA solution (25 μL) in DI water at a concentration of 53.2 μg mL^{-1} was added to an equal volume of LPEI or LPEI-*g*-PEG solution in DI water at N/P ratio 20. The mixture was vortexed and then incubated for 30 min at room temperature. To prepare crosslinked nanoparticles, siRNA was incubated with thiolated LPEI-*g*-PEG copolymer,[3] and then the nanoparticles suspension was transferred to a Biotech-grade RC float-dialyzer with MWCO of 3,500 Da and dialyzed against DI water for 24 h to oxidize thiol groups. The size and size distribution of nanoparticles were measured by dynamic light scattering (DLS) carried out on a Malvern Zetasizer Nano ZS90. TEM was performed on a FEI Tecnai 12 TWIN transmission electron microscope.

Gene silencing efficiency in cultured cells. PASMCs which stably express emerald green fluorescence protein (EmGFP) were seeded in 24-well tissue culture plate and incubated for 24 h to reach about 70% confluence, and then cells were transfected with PEI/siRNA, LPEI-*g*-PEG/siRNA or disulfide-crosslinked LPEI-*g*-PEG/siRNA nanoparticles carrying GFP-22 siRNA targeting EmGFP at the concentration of 100 nm in fresh DMEM containing 10% FBS without penicillin and streptomycin, and then change to 10% FBS-containing media after 4 h. Gene knockdown efficiencies were imaged under ZEISS 610 inverted fluorescence microscope, and cells were trypsinized and analyzed by FACSCalibur flow cytometer after 48 h. The cell proliferation WST-1 test was performed to assess cell proliferation and viability after 48 h of incubation.

RESULTS AND DISCUSSION

The use of PEG for nanoparticle surface functionalization had led to many favorable results due to its intrinsic physicochemical properties, such as low toxicity and immunogenicity. Nanoparticles functionalized with PEG chains have been described as long circulating drug delivery systems with potential applications for systemic drug administration. Moreover, PEG has been shown to substantially reduce nonspecific interactions with proteins through its hydrophilicity and

steric repulsion effects, thereby reducing opsonization and improving nanoparticle stability. In this study, we apply LPEI-*g*-PEG copolymer to siRNA delivery. First of all, we have confirmed that the LPEI-*g*-PEI copolymer can condense siRNA to form nanoparticles with high N/P ratio of 20. As shown in Figure 1, LPEI-*g*-PEG/siRNA nanoparticles exhibit more uniform size with an average diameter around 100 nm measured by DLS and TEM. Without PEG decoration, LPEI/siRNA nanoparticles will formed aggregates rapidly upon contact with serum-containing medium.

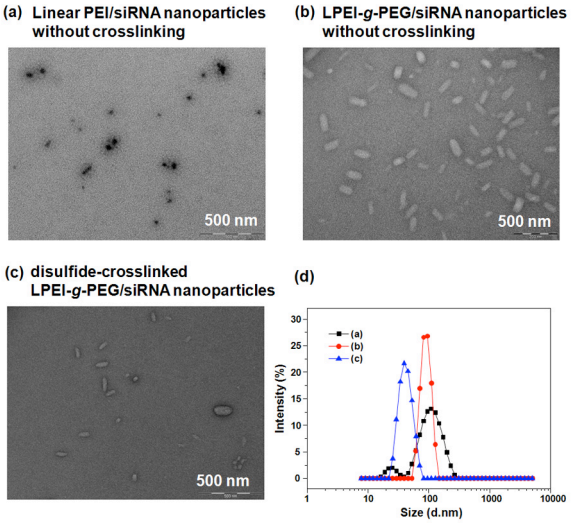

Figure 1. TEM images of linear PEI/siRNA nanoparticles (a), LPEI-g-PEG/siRNA nanoparticles without (b) and with disulfide-crosslinking (c). Size distributions of the three sets of particles were measured by dynamic light scattering (d).

Due to the short and rigid structure of siRNA in contrast with DNA, polycation/siRNA polyplexes usually exhibit poor stability in buffers at physiological ionic strength or in serum-containing media. In our study, the stability of LPEI-*g*-PEI/siRNA nanoparticle was enhanced by introducing disulfide bonds into the core of these nanoparticles. We have confirmed that LPEI-*g*-PEI/siRNA nanoparticle will dissociate during dialysis or in the present of 0.9% NaCl without crosslinking. Therefore, LPEI-*g*-PEI/siRNA nanoparticles after disulfide crosslinking exhibited smaller and more uniform morphology. The size of nanoparticles will play an important role in modulating cellular uptake and gene delivery efficiency.

We also test the gene knockdown efficiency mediated by LPEI-*g*-PEG/siRNA nanoparticles in PASMCs. As shown in Figure 2a, disulfide-crosslinked LPEI-*g*-PEG/siRNA nanoparticles under the tested condition decreased the endogenous GFP expression by 40%, which was significantly higher than non-crosslinked LPEI-*g*-PEG/siRNA nanoparticles. It was likely that more condensed and smaller nanoparticles obtained by this crosslinking method facilitated particle uptake by cells. When compared with LPEI/siRNA nanoparticles, which showed about 65% knockdown efficiency, the stealth effect of PEG segment located in LPEI-*g*-PEG/siRNA nanoparticles may decrease cellular association and internalization, and hence result in lower transfection efficiency. These unique properties justify further investigation on delivery efficiency to the lung *in vivo*. As shown in Figure 2b, none of the carriers tested show significant toxicity at the siRNA dose and culture conditions.

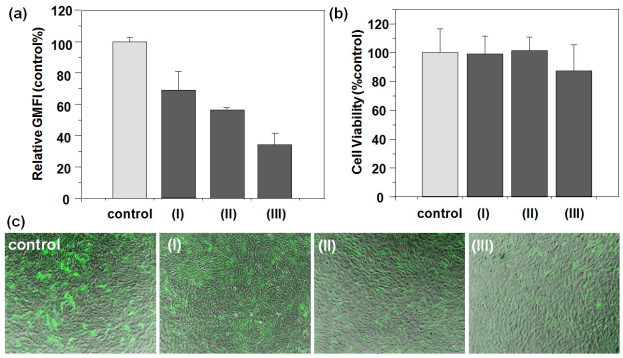

Figure 2. (a) Gene silencing efficiency of GFP-22 siRNA delivered by the three sets of particles in PASMCs were measured by FACS. (b) Cytotoxicity to PASMCs was determined by WST-1 assay. (c) Fluorescence images of PASMCs with GFP expression silenced by the three sets of particles. (I) LPEI-g-PEG/siRNA without crosslinking, (II) disulfide crosslinked LPEI-g-PEG/siRNA nanoparticles and (III) LPEI/siRNA nanoparticles.

CONCLUSION

LPEI-*g*-PEG copolymer was able to condense siRNA into more uniform nanoparticles and the stability of these nanoparticles can be enhanced by further disulfide crosslinking. Delivery of GFP-22 siRNA with disulfide crosslinked LPEI-g-PEG/siRNA nanoparticles significantly reduced the endogenous GFP expression in PASMCs, suggesting that these dual-sensitive nanoparticles can serve as an efficient gene delivery carrier.

REFERENCES

1. Luo D, Saltzman WM, *Nat. Biotechnol.* **2000**, 18, 33-37.
2. Boussif O, Lezoualch F, Zanta MA, Mergny MD, Scherman D, et al, *Proc. Natl. Acad. Sci.* U. S. A. **1995**, 92, 7297-7301.
3. King TP, Li Y, Kochoumian L, *Protein Conjugates* **1978**, 17, 1499-1506.

ACKNOWLEDGEMENT:

This study was supported by the Defense Threat Reduction Agency under the grant W81XWH-10-2-0053.

The American Society of Gene and Cell Therapy 15th Annual Meeting, Philadelphia, PA. May 15–19, 2012.

[647] Stabilized Quaternary Nanoparticles for Targeted Delivery of siRNA

Masataka Nakanishi, Deng Pan, Xuan Jiang, Hai-Quan Mao. Department of Materials Science and Engineering, Johns Hopkins University, Baltimore, MD; Translational Tissue Engineering Center, Johns Hopkins University, Baltimore, MD; Whitaker Biomedical Engineering Institute, Johns Hopkins University, Baltimore, MD

Target-specific systemic delivery using polyelectrolyte complex nanoparticles is a promising approach for siRNA delivery. However, polycation/siRNA complexes suffer from low stability in physiological media. In addition, the positive surface charge leads to serum protein adsorption, opsonization and non-specific uptake by macrophages. An effective stabilization, passivation and targeting strategy is essential to the success of polycationic nanoparticle-mediated siRNA delivery. We have recently reported that sodium triphosphate (TPP) as an anionic stabilization agent can significantly improve the stability of polycation/siRNA nanoparticles and results in enhanced gene knockdown. Here, we show that these TPP-stabilized siRNA nanoparticles can be coated by hyaluronic acid (HA) to further improve their colloidal stability in serum containing medium. This strategy is applicable to several polycations used to condense siRNA, including branched and linear polyethylenimine (BPEI and LPEI). BPEI or LPEI were used to condense siRNA in the presence of TPP according to the method we reported previously, followed by coating with HA. These two sets of nanoparticles exhibited spherical (80-180 nm) and highly uniform morphology (Fig. 1). Both TPP crosslinking and HA-coating are essential to maintaining the high complex stability and colloidal stability for these nanoparticles. In the absence of TPP stabilization, irregular shaped, large aggregates were obtained when BPEI/siRNA complexes were coated with HA. The quaternary nanoparticles showed increased stability in a solution with the physiological ionic strength and serum condition.

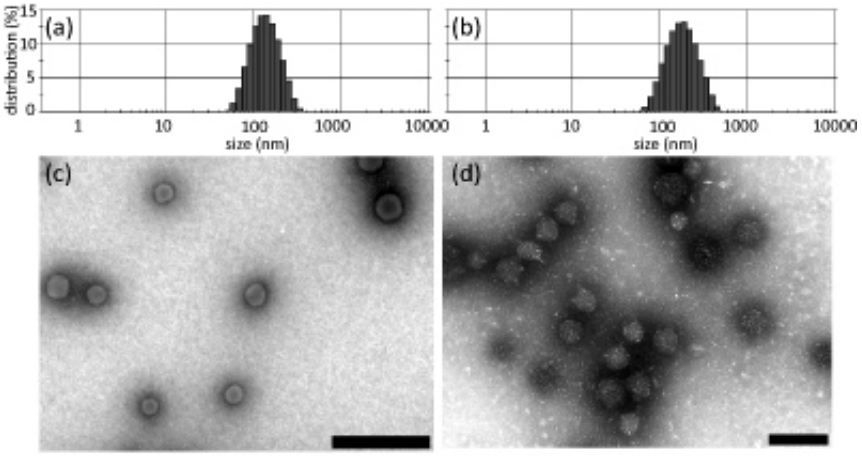

Figure. 1 Size distribution and TEM images of TPP-stabilized quaternary nanoparticles formed from BPEI (a, c) and LPEI (b,d) (scale bar = 500 nm).

Using dual luciferase assay, we have shown that gene silencing efficiency of HA-coated siRNA nanoparticles was enhanced by co-condensation with TPP for both BPEI and LPEI in serum-containing media, compared with that of nanoparticles without TPP (Fig. 2). The results highlight the effectiveness of TPP-co-condensation as a useful strategy to improve the gene silencing efficiency of HA-coated siRNA nanoparticles.

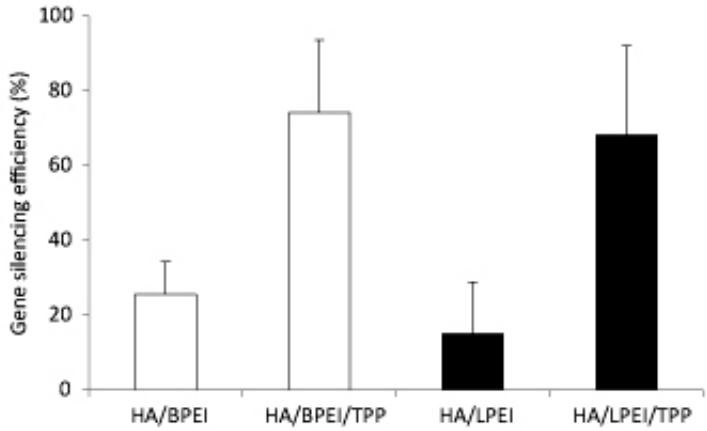

Figure. 2 Gene silencing efficiency mediated by siRNA nanoparticles in HeLa cells in the presence of 10 % serum. A siRNA dose of 100 nM was used in all transfection groups. Values are expressed as Mean +SEM (n = 4).

Keywords: RNAi and shRNA; Non-Viral Gene Delivery; Synthetic Gene Delivery Systems

Date: Saturday, May 19, 2012
Session Info: Poster Session: Chemical and Molecular Conjugates II (5:15 PM-7:15 PM)
Presentation Time: 5:15 pm
Room: Hall A

Close Window

American Society of Gene and Cell Therapy 14th Annual Meeting, Seattle, Washington, USA, May 18-21 2011.

Enhanced Stability and Knockdown Efficiency of Block Copolymer/siRNA Micelles by Co-condensation with Sodium Triphosphate

Masataka Nakanishi[1,5,*], Rajesh Patil[1,*], Yong Ren[1], Rishab Shyam[2], Philip Wong[3] and Hai-Quan Mao[1,2,4,5]

[1]Dept. of Materials Science and Engineering, [2]Dept. of Biomedical Engineering, [3]Dept. of Neuroscience, [4]Whitaker Biomedical Engineering Institute, [5]Translational Tissue Engineering Center , Johns Hopkins University, Baltimore, MD USA

Background

A. RNA Intereference (RNAi)

RNA interference (RNAi) is a highly evolutionarily conserved mechanism of gene regulation. The classic RNAi occurs at the post-transcriptional level and is triggered by short double-stranded RNA (dsRNA) also known as short interfering RNA (siRNA) which is processed from long dsRNA by the RNase III enzyme Dicer or introduced into a cell exogenously. After being loaded into the so-called RNA-inducing silencing complex (RISC) in the cytoplasm, the siRNA would causes sequence-specific degradation of its homologous mRNA sequences. RNAi was first discovered in 1998 by Andrew Fire and Craig Mello in the nematode worm Caenorhabditis elegans and later found in a wide variety of other organisms, including mammals.

B. Polyelectrolyte complex nanoparticle

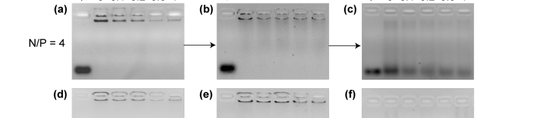

- Nano-sized particle (Diameter : 100-300 nm)
- Colloidal stablity in physiological condition.
- Delivery of negative charged genes through cell membrane
- Higher protection of incorporated gene against enzymatic degradation
- Prolonged blood circulation

C. Problems of siRNA-loaded polyelectrolyte complex

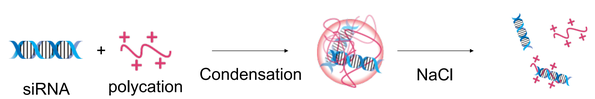

siRNA-loaded complex suffers from low stability under physiological condition probably due to the short and rigid structure of siRNA in contrast to plasmid DNA.

D. Tripolyphosphate (TPP) as ionic crosslinker

Tripolyphosphate (TPP)

- ionic gelation agent
- Approved by FDA

TPP has been used as an effective cross-linking agent for polycations (e.g. chitosan) because of its non-toxic nature.

Hypothesis: Similar crosslinking can form between TPP and gene carrier, thus facilitating condensation with siRNA and increasing stability of nanoparticle.

Materials

A. Scheme

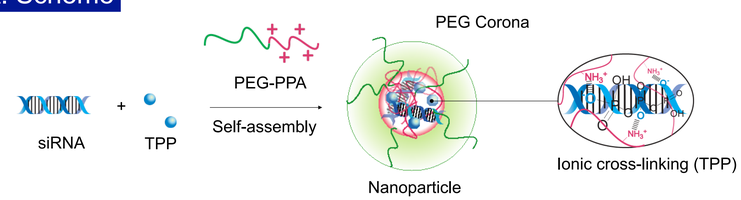

Ternary complex nanoparticles were prepared by various P'/N ratios for N/P ratios of 4 and 8.

<Definition>
N/P = [Amine of PPA]/[Phosphorus of siRNA]
P'/N = [Phosphorus of TPP]/[Amine of PPA]

B. Polymeric Carrier

Poly(ethylene glycol)-*block*-polyphosphoramidate (PEG-PPA)

M_w = 12k-38k, M_w/M_n = 1.5

C. Nanoparticle Formation

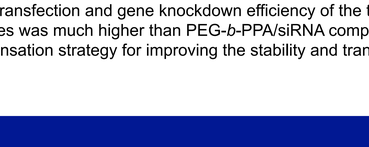

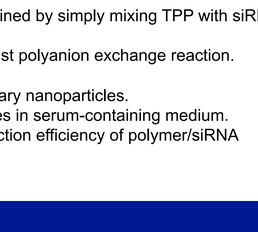

Fig. 1 (left) Dynamic light scattering histgram of nanoparticles (P'/N = 0.2 for N/P 4). (right) TEM images of nanoparticle formed at P'/N of 0 and 0.5 for N/P of 4 and 8.

Physicochemical Properties of Nanoparticles Cross-linked by TPP

Complex Stability of Nanoparticles

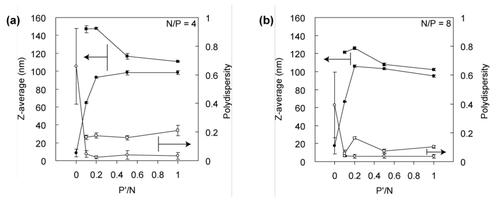

Fig. 2 The z-average (left ordinate) and PDI (right ordinate) measured by dynamic light scattering analysis of nanoparticles formed at various P'/N ratios and N/P ratios of 4 (a) and 8 (b), respectively, before (filled circle, empty circle) and after (filled square, empty square) incubation with 150 mM NaCl for 24 h. Values represent Mean ± SEM (n=3). Particles without TPP crosslinking dissociated after incubation in 150 mM NaCl; therefore, no data points were included for P'/N=0 for salt incubation lines (filled square, empty square) here.

Zeta-potential

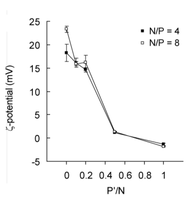

Fig. 3 Zeta-potential of nanoparticles prepared at various P'/N ratios for N/P ratios of 4 (filled square) and 8 (empty square), respectively. Values represent Mean ± SEM (n=3).

Nanoparticle Stability in 50% Serum

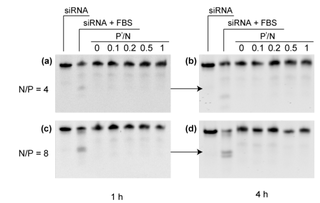

Fig. 4 Gel retardation assay of siRNA integrity in nanoparticles against enzymatic degradation in 50% FBS. Nanoparticles prepared at various conditions were incubated in 50% FBS for 1 h (a and c) and 4 h (b and d), respectively.

Complex Stability Against Challenge by Polyanions

Fig. 5 Gel retardation assay of complexation efficiency for siRNA at various P'/N ratios for N/P ratios of 4 and 8, respectively. Nanoparticles prepared at various conditions were incubated with polyvinylsufate for 1 and 5 h at 37 °C at a molar ratio of sulfate groups in polyvinylsufate to phosphate groups in siRNA of 5.

M. Nakanishi et. al., *Pharm. Res.* (2011)

Transfection and Knockdown Efficiency / Cell viability

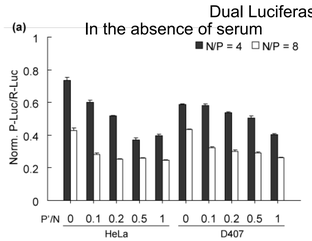

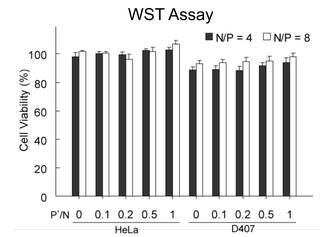

Fig. 6 Gene silencing efficiency mediated by PEG-PPA/siRNA(against firefly)/TPP ternary nanoparticles at various P'/N ratios for N/P ratios of 4 and 8 in HeLa and D407 cells in the absence (a) and presence (b) of 10% serum. A siRNA dose of 100 nM was used in all transfection groups. Values are expressed as Mean ± SEM (n=4).

Fig. 7 Viability of HeLa and D407 cells transfected with PEG-PPA/siRNA/TPP ternary nanoparticles in 10% serum-containing medium under the conditions described in Fig 5. Values are expressed as Mean ± SEM (n=4).

Conclusion

- Co-condensation with TPP was a safe and effective approach to improve the complex stability and gene silencing efficiency of PEG-*b*-PPA/siRNA complex nanoparticles.
- Spherical ternary nanoparticles with smaller size (80 - 100 nm) and narrower distribution (PDI < 0.01) were obtained by simply mixing TPP with siRNA before condensing with PEG-PPA.
- These ternary nanoparticles showed improved complex stability in salt and serum-containing medium and against polyanion exchange reaction.
- The stability of ternary nanoparticles increased with increasing P'/N and N/P ratios.
- The improved stability correlated well with the enhanced transfection and gene knockdown efficiency of the ternary nanoparticles.
- The knockdown efficiency of TPP-crosslinked nanoparticles was much higher than PEG-*b*-PPA/siRNA complexes in serum-containing medium.
- These results highlight the effectiveness of TPP co-condensation strategy for improving the stability and transfection efficiency of polymer/siRNA nanoparticles.

Acknowledgments

The presenters thank Dr. James F. Dillman III and Dr. Albert L. Ruff at the Cell and Molecular Biology Branch, US Army Medical Research Institute of Chemical Defense, and Dr. Xuan Jiang at Department of Materials Science and Engineering, Johns Hopkins University, for discussions throughout the study. We thank Dr. Noriko Esumi for providing D407 cells. This study was supported by US Army Defense Threat Reduction Agency through the Grant W81XWH-10-2-0053.